# Journal Pre-proof


Eukaryotes in soil aggregates across conservation managements: Major roles of protists, fungi and taxa linkages in soil structuring and C stock

Elisa Pellegrino, Gaia Piazza, Thorunn Helgason, Laura Ercoli

PII: S0038-0717(21)00337-0

DOI: https://doi.org/10.1016/j.soilbio.2021.108463

Reference: SBB 108463

To appear in: *Soil Biology and Biochemistry*

Received Date: 22 May 2021

Revised Date: 13 October 2021

Accepted Date: 15 October 2021

Please cite this article as: Pellegrino, E., Piazza, G., Helgason, T., Ercoli, L., Eukaryotes in soil aggregates across conservation managements: Major roles of protists, fungi and taxa linkages in soil structuring and C stock, *Soil Biology and Biochemistry* (2021), doi: https://doi.org/10.1016/j.soilbio.2021.108463.

# Eukaryotes in soil aggregates across conservation managements: major roles of protists, fungi and taxa linkages in soil structuring and C stock

**Running title: eukaryotic diversity and roles in soil aggregates**

Elisa Pellegrino[1,*,+], Gaia Piazza[1,+], Thorunn Helgason[2], Laura Ercoli[1]

[1]Institute of Life Sciences, Scuola Superiore Sant'Anna, Pisa, Italy and [2]Department of Biology University of York, York, UK

[+]These authors contributed equally: Elisa Pellegrino, Gaia Piazza

*Elisa Pellegrino elisa.pellegrino@santannapisa.it

## Abstract

The stabilization of soil organic carbon (SOC) promoted by conservation agriculture (CA) depends on soil aggregation. Aggregation protects SOC and creates heterogeneous microhabitats hosting diverse soil biota which in turn promote aggregation. A long-term experiment, studying the interaction of tillage with nitrogen (N) fertilization on a soybean-wheat rotation, was used to investigate eukaryotic community diversity, composition, and structure within small macroaggregates (sM) and occluded microaggregates (mM). Using high-throughput Illumina sequencing, we found (i) a different eukaryote diversity response to management intensification across soil aggregates and soil depths; (ii) a conserved core community composition of eukaryotes across CA treatments and aggregates at surface and subsurface layers; (iii) a different effect of tillage on eukaryotic community structure in sM and mM along the soil profile according to N availability; (iv) a positive association of protists, and fungi with the amount of sM and mM, and their SOC content; (v) a stronger complexity of within- and cross-domain networks (eukaryotes and eukaryotes-prokaryotes) in mM than in sM at surface layer. Overall, our findings demonstrated for

the first time that protists together with fungi play major roles in soil structuring and C cycling, and that Cercozoa represent hubs in soil biota aggregate networks.

**Keywords**

soil aggregates; soil eukaryotes; protists; Illumina sequencing; 18S rRNA gene amplicon; soil biota linkages.

## 1. Introduction

Soil organic carbon (SOC) stability mainly depends on physical protection (Six et al., 2000; Six and Paustian, 2014), whereas molecular structure of plant residues and root exudates play a secondary role in SOC persistence (Schmidt et al., 2011; Lal et al., 2015). Organic carbon (C) is protected in soil aggregates by physically limiting the access of decomposers and enzymes and the diffusion of $O_2$.

According to the model of Tisdall and Oades (1982), primary particles (clay and silt particles, Ø <53 µm) are bound together by persistent bacterial, fungal, and plant debris into free microaggregates (Ø 53-250 µm). Free microaggregates are bound into macroaggregates (Ø > 250 µm) by transient agents (i.e., microbial and plant polysaccharides) that are rapidly decomposed by microorganisms, and by temporary agents (i.e., roots, fungal hyphae and glomalin) that persist in the medium term. Labile SOC is mainly located in macroaggregates, while free microaggregates contain a more recalcitrant SOC pool (Elliott, 1986; Jastrow and Miller, 1998).

Intensive agricultural practices, such as tillage and fertilization, shorten the life cycle of macroaggregates and diminish the formation rate of new microaggregates, worsening soil structure (Six et al., 2000). In no-tillage systems (NT), the slower turn-over of macroaggregates resulted in more sequestration of crop-derived C in microaggregates formed within macroaggregates (occluded microaggregates, mM; Ø 53-250 µm), and thus the amount of mM is crucial for the long-term C-sequestration in soils (Six et al., 2000; Denef et al., 2007; Sheehy et al., 2015). In this context, the application of conservation agriculture (CA) practices (i.e., minimum tillage/NT, crop rotation and mulching) may allow the establishment of microhabitats with variable nutrient availabilities for a diverse soil biota, acting as efficient binding agent (Kong et al., 2011; Gupta and Germida, 2015; Totsche et al., 2018; Piazza et al., 2019). Moreover, CA practices may also produce yields equivalent to or even greater than conventional systems (Rusinamhodzi et al., 2011; Aune, 2012; Pittelkow et al., 2015; Himmelstein et al., 2016).

In boreal climates, long-term NT and minimum tillage (MT) have been shown to increase the amount of macroaggregates and mM as well as their SOC content in the shallow layer (surface soil within horizon A) in comparison to conventional tillage (CT) (Franzluebbers and Arshad, 1997; Sheehy et al., 2015). This was demonstrated under various soil textures and was more evident in clay, clay-loam and silt-loam soils. Similarly, in humid tropical climates and sandy loam soils, long-term application of MT significantly increased SOC content in large soil aggregates, whereas the reverse was reported under CT (Onweremadu et al., 2007). Accordingly, Denef et al. (2007) highlighted a promotion of mM fraction and mM-associated C stocks in NT and MT compared with CT under similar climate. Moreover, nitrogen (N) fertilization was reported to increase SOC in macroaggregates and free microaggregates by decreasing the activity of cellulolytic fungi and bacteria (Ghosh et al., 2019; Duan et al., 2021). Recently, in a cold and humid Mediterranean area and in a silt-loam soil, high N fertilization rates in combination with MT not only increased mM, but also promoted a shift to low level, but more efficient C-cycling microbial enzyme activities, which were correlated to a greater accumulation of SOC (Piazza et al., 2020). Overall, in four regions across Europe the intensification of agriculture was reported to consistently reduce soil biota diversity in bulk soil, making soil food webs less diverse and composed of smaller bodied organisms (Tsiafouli et al., 2015).

Although the role of bacterial and fungal communities (including arbuscular mycorrhizal fungi, AMF) in soil aggregation and SOC stabilization is widely recognized to be fundamental (Six et al., 2004; Lehmann et al., 2017; Bach et al., 2018), the diversity and potential role of other soil biota have received less attention. Soil biota diversity has indeed proved to be the major driver of C sequestration and nutrient cycling in bulk soil (De Vries et al., 2013; Wagg et al., 2019; Delgado-Baquerizo et al., 2020). Many studies demonstrated that earthworms and bacterivore nematodes are directly involved in the formation of macroaggregates by incorporating fresh organic matter inside mM and thus promoting SOC accumulation (Six et al., 2004; Pulleman et al., 2005; Bossuyt et al., 2006; Fonte et al., 2007; Zhang et al., 2013; Delgado-Baquerizo et al., 2020). Moreover, an indirect

84 effect on SOC accumulation by earthworms and bactrivorous nematodes was also reported and
85 explained by the shift of soil microbial diversity through taxa regulating nutrient flow (Delgado-
86 Baquerizo et al., 2020). Thus, in this study, we investigate the diversity and related roles of the
87 eukaryotic component of soil biota within small macroaggregates (sM) and mM across CA
88 managements. Moreover, since a more connected soil biota network takes up more C (Morriën et
89 al., 2017), the study was extended to elucidate how eukaryotes are connected among each other, and
90 to the prokaryotic community. In this context, long-term CA field experiments in the Mediterranean
91 area, such as the one used in this study, provide a great opportunity for improving the understanding
92 of soil eukaryotic diversity and functionality in soil aggregates and C stocks.

93 The following hypotheses were tested: (1) conservation tillage and N fertilization shift soil
94 eukaryote community diversity, composition and structure, in soil aggregates along the soil profile;
95 (2) soil aggregates differentially shape the diversity, composition and structure of soil eukaryotes;
96 (3) some eukaryotic taxa are predictors for soil structuring and C stocks; (4) eukaryotes form
97 structured assemblages and distinctive networks in soil aggregates (within-domain networks); (5)
98 the traits of the eukaryotes-prokaryotes networks vary across aggregates (cross-domain networks),
99 and some network traits can predict soil structuring and C stocks.

100

101 **2. Materials and Methods**

102 *2.1. Field experiment*

103 A long-term CA field experiment on a bread wheat (*Triticum aestivum* L.) - soybean (*Glycine*
104 *max* L. Merr.) rotation was set up in 1993 at the Centro Interdipartimentale di Ricerche Agro-
105 Ambientali Enrico Avanzi (Pisa, Italy; 43°40' latitude N; 10° 19' longitude E; 1 m above sea level)
106 in an alluvial silt loam soil (131, 613 and 256 g $kg^{-1}$ of sand, silt and clay, respectively). The
107 experiment was conducted comparing two tillage intensities and two N fertilization levels. The
108 tillage intensities were: conservation tillage (minimum tillage, MT: disk harrowing at 15-cm depth)

and conventional tillage (CT: mouldboard ploughing at 25-cm depth, disking and harrowing at 15-cm depth). The N fertilization levels applied only to bread wheat were: 0 and 200 kg N $ha^{-1}$ (N0 and N200, respectively). The soil is classified as Typic Xerofluvent by USDA system (Soil Survey Staff, 1975) and as Fluvisol by FAO (IUSS, 2006). Climate of the site is cold, humid Mediterranean (Csa), according to the Köppen-Geiger climate classification (Kottek et al., 2006). The experiment was arranged following a split-plot design, with tillage as main-plot factor and N fertilization as subplot factor and three replicate plots (dimension: 11.5 x 14.5 m). The N fertilizer treatment was applied as urea and the rate was split into three applications, before sowing (60 kg N $ha^{-1}$), at the first detectable node (70 kg N $ha^{-1}$), and 15 days after this stage (70 kg N $ha^{-1}$). Under CT, almost 100% of the residues were incorporated in the 0-25 cm soil layer, whereas under MT approximately 50% of the crop residues were incorporated at 0-15 cm depth. Crops were managed applying pre-emergence herbicide for weed control and no disease or insect treatments (Piazza et al., 2020).

.

*2.2. Soil sampling and analysis of soil physical and chemical parameters*

Soil sampling was carried out in Spring 2016 before soybean sowing. In each replicate plot, a homogenized sample was obtained by mixing four soil cores collected at two soil depths (surface layer: 0-15 cm; sub-surface layer: 15-30 cm). A total of twenty-four soil samples were collected (12 at the surface layer; 12 at the subsurface layer). Once in the laboratory, each sample was air-dried, gently broken apart and then passed through an 8-mm sieve. The isolation of small macroaggregates (sM; 250-2000 µm) was done from 80 g of the sieved soil samples by the wet sieving method (Six et al., 1999). Occluded microaggregates (mM; 53-250 µm) were isolated from an additional isolation of sM (i.e., starting from 80 g of the sieved soil samples) and utilising a device designed and built by Piazza et al. (2020). Once collected, the fractions were freeze-dried (FreeZone 2.5 Labconco, Kansas City, MO, USA) for 48-72 h for dry weight determination and chemical and molecular analyses. Both aggregate fractions of all samples were then analysed for SOC by CHN

combustion method (LECO, Italy) and SOC content was calculated and expressed in Mg $ha^{-1}$ (Bremner and Mulvaney, 1982; Piazza et al., 2020).

*2.3. Molecular analyses*

DNA was extracted from 0.25 g of sM (n=24) and mM samples (n=24) using the DNeasy PowerSoil Kit (QIAGEN, Venlo, Netherlands). The DNA extracts were then quantified by a spectrophotometer (NanoDrop Technology, Wilmington, DE) and stored at -20 °C. PCRs were generated from 10 ng $\mu L^{-1}$ genomic DNA in volumes of 25 µL with 0.125 U $\mu L^{-1}$ of GoTaq® Hot Start Polymerase (Promega Corporation, WA, USA), 0.5 µM of each primer, 0.2 mM of each dNTP, 1 mM of $MgCl_2$ and 1x reaction buffer, using the PTC-200 96-well Peltier Thermal Cycler (MJ Research, MA, USA). The primers were TAReuk454FWD1-ill (5'-TCGTCGGCAGCGTCAGATGTGTATAAGAGACAGANNNHNNNWNNNHCCAGCASCYGC GGTAATTCC-3') and TAReukREV3-ill (5'-GTCTCGTGGGCTCGGAGATGTGTATAAGAGACAGTACTTTCGTTCTTGATYRA-3') (modified from Stoeck et al., 2010). The primer pair has attached Illumina sequencing tags, and for the forward primer a 13 bp random sequence was included in order to improve cluster definition on the MiSeq slide. Primers target the hypervariable region V4 of the small subunit ribosomal RNA (SSU rRNA 18S) gene fragment. The thermal cycler was programmed as follows: 95 °C for 2 min, 35 cycles at 94 °C for 30 s, 50 °C for 45 sec, 72 °C for 1 min and 30 s and a final extension step at 72 °C for 10 min. PCR products were examined by electrophoresis through a 1% agarose gel in 0.5 × TBE buffer, then purified with magnetic beads (Agencourt® AMPure® XP, Beckman Coulter, USA) and freshly prepared 80% ethanol, and quantified by fluorimetry with the use of Quant-iT™ dsDNA HS (High-Sensitivity) Assay Kit (Invitrogen by Thermo Fisher Scientific, CA, USA), following the instructions of the manufacturer. Cleaned and quantified amplicons of each library were adjusted in an equimolar ratio (10 ng/µL) for the required Illumina P5 and P7 sequences

addition along with index sequences in a new PCR step. Indexing was performed using primers from the Nextera® Index kit (sets A and D; Illumina Inc., CA, USA) and the resulting metabarcoding libraries were sequenced on an Illumina MiSeq sequencer (2 * 300 bp paired-end reads) at the Genomics and Bioinformatics Laboratory (Technology Facility, Department of Biology, University of York, UK). Details are given in the Supplementary Methods 1.

*2.4. Bioinformatic analyses*

Raw data generated from the Illumina MiSeq sequencing run were processed and analyzed following the pipelines of QIIME 2 (2018.4) and USEARCH (v10.0.240) (Edgar, 2010; Caporaso et al., 2012). Forward and reverse paired-end sequences were assembled independently for each sample using -fastq_mergepairs USEARCH command. Primer sequences were then trimmed off by employing cutadapt plugin (2018.4) with default settings. To avoid potential errors in sequencing data, quality of sequence reads was checked by -fastq_eestats2 USEARCH command, using the expected number of errors in a read as a measure of quality for filtering (Edgar and Flyvbjerg, 2015). Reads were then trimmed at the length where the "drop-off" point for the maximum expected error value occurred (250 bp). Quality filtered reads were de-replicated by -fastx_uniques USEARCH command, then Operational Taxonomic Units (OTUs) were generated using USEARCH by clustering sequence reads at the 97% similarity threshold. During the process, chimeric sequences and singletons were removed from the dataset. For the curation, the sequences were aligned using ClustalW and then Neighbor Joining (NJ) phylogenetic tree was built in MEGA7 (Kumar et al., 2016) (https://www.megasoftware.net). The most abundant sequence of the eukaryotic OTU in each cluster was selected, and used as representative sequence for that OTU after branch collapsing. For the curation, the sequences were aligned using ClustalW and then Neighbor Joining (NJ) phylogenetic tree was built in MEGA7 (Kumar et al., 2016) (https://www.megasoftware.net). The most abundant sequence of the eukaryotic OTU in each

cluster was selected, and used as representative sequence for that OTU after branch collapsing. The OTUs were phylogenetically assigned using the 18S SSU SILVA database (version 132, release date 13.12.2017) (Quast et al., 2012; Yilmaz et al., 2013) by clustering sequence reads at the 97% similarity threshold. After curation, the representative sequences were re-aligned using ClustalW and the phylogenetic tree was built in MEGA7 using the Neighbor Joining (NJ) analysis with 1 000 boostrap replicates and the Kimura 2-parameter model (uniform rates).

The suitability of the eukaryotic community sampling was verified by rarefaction curves plotting the number of eukaryotic classes/phyla *versus* the number of sequence reads, while accumulation curves were calculated plotting the number of classes/phyla *versus* the number of soil samples using the package Vegan in R (Oksanen et al., 2013). Since there was a high variability in the number of reads per sample, sequencing depth per sample was standardized to the median number of reads across the samples in each data matrix using the same package in R (standardized datasets). All representative sequences were deposited in the NCBI GenBank database (SUB5948379 submission: MN178662-MN178794 accession numbers).

Prokaryotic data were obtained from the same soil matrices and depths (Piazza, 2019) and were based on the V4 region of the 16S rRNA gene sequenced using a MiSeq Illumina approach (SUB5941754 submission: MN171543-MN172157 accession numbers).

### *2.5. Statistical analyses*

To test hypothesis 1 - Conservation tillage and N fertilization shift soil eukaryote community diversity, composition and structure in soil aggregates along soil profile - analysis of variance (ANOVA), Venn diagrams and permutational analysis of variance (PERMANOVA) were applied. Concerning diversity, richness, Shannon index (*H'*) and Simpson index ($\lambda = 1- \lambda'$) were calculated at class level and analysed by two-way ANOVA, according to the experimental design. These analyses were done in Vegan package in R and plotted by ggplot2 (Wickham and Chang, 2008).

Data were ln--transformed when needed to fulfil the assumptions of ANOVA. Post-hoc Tukey-B significant difference test was used for comparison among treatments. Concerning composition, Venn diagrams were drawn to visualize the OTUs unique to the treatments as well as the shared ones. The standardized datasets were used to generate the Venn diagrams by the online tool InteractiVenn (http://www.interactivenn.net; Heberle et al., 2015). Concerning structure, the relative abundances of eukaryotes were calculated at class level and the permutational analysis of variance (PERMANOVA) (Anderson and Braak, 2003) and the analysis of homogeneity of multivariate dispersion (PERMDISP) were used to test the effect of treatments (Togerson, 1958; Clarke and Gorley, 2006). Response data were square-root transformed to down-weight the dominant taxa and the Bray-Curtis index of dissimilarity was used to measure ecological distance. When PERMANOVA indicated a significant effect, the principal coordinate analysis (PCO) was carried out (Anderson et al., 2008) to visualize the most relevant patterns in the response data. In each PCO biplot, only the taxa with a strong correlation (r = 0.50-0.80) with the ordination scores on each PCO axis were displayed. *P*-values were calculated using the Monte-Carlo test and residuals were permuted according to the experimental model (Oksanen et al., 2013). Multivariate analyses were performed using PRIMER 6 and PERMANOVA+ software (Clarke and Gorley, 2006; Anderson et al., 2008).

To test hypothesis 2 - Soil aggregates differentially shape the diversity, composition and structure of soil eukaryotes - eukaryotic richness, *H'* and λ at phylum level and at both soil depths were analysed by one-way ANOVA, using soil matrix (sM *vs* mM) as fixed factor, and tillage and N fertilization as covariates. Analyses were performed in Vegan package in R and data were plotted by ggplot2. Data were ln-transformed when needed to fulfil the assumptions of ANOVA, and the post-hoc Tukey-B significant difference test was used for comparison among treatments. Moreover, the effect of matrix on composition and structure were analysed at phylum level using the Venn diagrams and PERMANOVAs, as described above.

To test hypothesis 3 **-** Some eukaryotic taxa are potential predictors for soil structuring and C stocks - multiple regression analysis was applied using as independent variables the standardized relative abundances (calculated as described above) of eukaryotic taxa at class level. To account for the compositional nature of the data, an additive log-ratio transformation was applied (Gloor et al., 2017). The dependent variables were sM and mM weights, and SOC content per unit of surface in sM and mM. The assumptions of the linear regression model were verified (Supplementary Method 2) and the multiple linear regression analysis was applied using a stepwise method with the following probability criteria: $P < 0.05$ to accept and of $P > 0.05$ to remove a phylum or a within/cross-domain network traits. Multiple regressions were performed using the SPSS software package version 25.0 (SPSS Inc., Chicago, IL, United States)**.** Details about regression analysis are reported in Supplementary Methods 2.

To test hypothesis 4 - Eukaryotes form structured assemblages and distinctive networks in soil aggregates - we built networks using the SParse InversE Covariance estimation for Ecological ASsociation Inference (SPIEC-EASI) package version 0.1 in R (https://github.com/zdk123/SpiecEasi/). SPIEC-EASI is a pipeline for inferring sparse inverse covariance matrix within and between multiple compositional datasets, under joint sparsity penalty (Kurtz et al., 2015). The within-domain analyses were performed on the standardized eukaryotic dataset at class level for each soil matrix and depth. The neighborhood selection (MB method) was applied as graphical inference model (Meinshausen and Bühlmann, 2010), since it has been shown to better perform than other available methods (e.g., CCREPE, SPARCC, SPIEC-EASI glasso) (Kurtz et al., 2015). The Stability Approach to Regularization Selection (StARS) was applied to select the optimal sparsity parameter (Liu et al., 2010), and the StARS variability threshold was set to 0.05 and $n\lambda$ to 100 for all networks. We evaluated the weights of the edges in the networks using SPIEC-EASI (frequency *versus* edge weights = modularity), and we plotted the degree distributions of frequencies of the edges using adj2igraph (Kurtz et al., 2015). In the networks a node represents a connected taxon, an edge the connection between taxa, a singleton an unconnected taxon and a

dyad two connected taxa. For the eukaryotic networks (within-domain network) we calculated the following parameters: number of nodes excluding singletons, number of edges, number of singletons and dyads, number of subnetworks (a subnetwork is a network composed by at least three nodes), mean nodes per subnetwork, linkage density (complexity: the average number of edges per node), percentage of positive interactions and modularity. Moreover, in each network, we calculated the frequency of the phyla within the subnetworks, the mean of edges and nodes, and the percentage of positive edges for each phylum. Details about trait calculations are given in Supplementary Methods 3.

To test hypothesis 5 - The traits of the eukaryotes-prokaryotes networks vary across aggregates we inferred the associations between eukaryotes and prokaryotes domains by the cross-domain extension of SPIEC-EASI (Kurtz et al. 2015; Tripton et al., 2018). The same traits calculated for within-domain networks, except for the positive edges, were assessed (Supplementary Methods 3). In addition, the percentage of eukaryotes/prokaryotes per subnetwork was calculated and the number of subnetworks with only eukaryotes, only prokaryotes and with both domains were counted. The significance of the cross-domain relationships was tested by the Mantel test (Mantel and Valand, 1970) on the standardized read data that were centered and normalized and using the function Jaccard in PC-ORD 5 to build the resemblance matrix (Grandin, 2006) and also by the co-Correspondence Analysis (CoCA) (ter Braak and Schaffers, 2004) in CANOCO 5 (ter Braak and Smilauer, 2012). To test if some network traits can predict soil structuring and C stocks - a multiple linear regression was performed after verification of the assumptions (Supplementary Methods 3). The analysis was performed using as independent variables the log(1+x)-transformed and normalized within- and cross-domain network traits in sM and mM (i.e., traits of eukaryotic networks and of eukaryotic-prokaryotic networks), and using as dependent variables sM and mM weights, and SOC content per unit of surface in sM and mM. Scripts for within and cross-domain network construction and analysis are available in Supplementary Methods 4.

## 3. Results and discussion

### *3.1. Illumina sequencing information*

MiSeq sequencing yielded a total number of 2 940 322 reads from the 48 soil samples, and following quality-filtering a total of 2 884 052 sequence reads having a length of 392 bp were obtained. After BLAST against the 18S SSU SILVA database (Quast et al., 2012; Yilmaz et al., 2013), we found 2 036 277 reads, ranging from 3 to 106 540 reads per sample that were assigned to a total of 4 211 OTUs. After sequence curation and the removal of Plantae sequences, 863 809 reads, ranging from 6 421 and 46 429 reads per sample, were retrieved and assigned to 133 OTUs, 56 classes and 27 phyla (Fig. S1, Fig. S2). The rarefaction and accumulation curves demonstrated that sampling effort was sufficient as the curves reached the asymptote (Fig. S3, Fig. S4).

### *3.2. Effect of conservation management on eukaryotic diversity in soil aggregates*

To test if conservation tillage and N fertilization shift the diversity of soil eukaryotes in soil aggregates (hypothesis 1), richness and diversity indices were determined along the soil profile in small macroaggregates (sM) and occluded microaggregates (mM). A greater eukaryotic diversity in sM was consistently found at both soil layers under CT compared to MT, as shown by the significant increase of richness (+26%) and *H'* and λ (+9%) (Fig. S5). This higher eukaryotic diversity might be due to larger root development and higher availability of root exudates, organic matter (e.g., nutrients, organic acids), water and oxygen, reported under deep ploughing systems, and which have been shown to promote microbial growth and soil biota diversity/functionality (Guan et al., 2014; Edwards et al., 2015; Ercoli et al., 2017; Piazza et al., 2020), according to the response of individual taxonomic units to habitat and trophic conditions (van Capelle et al., 2012). At surface layer, N fertilization significantly increased λ under MT, suggesting an increase in number of relative abundances of taxa regulated by N availability. Conversely, under CT, λ was

311 high and not modified by N fertilization, suggesting non-limiting N availability due to improved
312 plant growth and higher mineralization rate of residues. A low eukaryotic diversity was previously
313 found in bulk soil under N fertilization (Lentendu et al., 2014), and within soil aggregates a higher
314 microbial diversity was found at low nutrient availability and NT compared with high nutrient
315 availability and ploughing (Lagomarsino et al., 2012; Zhang et al., 2013; Bach et al., 2018).

316 In mM an opposite pattern was found at surface layer, and no effect of N fertilization alone or
317 in interaction with tillage was observed at both soil depths (Fig. S5). At surface layer, the
318 eukaryotic diversity indices increased by 6% under MT compared to CT. Under tillage
319 intensification, macroaggregates are indeed disrupted and occluded microaggregates became free in
320 the soil (Six et al., 2000), potentially reducing diversity and C sequestration. This is supported by
321 the highest SOC accumulation observed in mM under MT (Piazza et al., 2020), and by the high soil
322 biota diversity found in the present study within mM.

323 To test if soil aggregates differentially shape the diversity of soil eukaryotes (hypothesis 2),
324 richness, *H'* and λ were determined in sM and mM. Overall eukaryotic diversity was significantly
325 higher in mM than in sM (Fig. S5) (i.e., at surface layer: richness +16%, *H'* +6%, and λ +2%; at
326 subsurface layer: richness +20 and *H'* +5%). These results are in accordance with the higher
327 richness and *H'* of bacteria and fungi found in free microaggregates compared to large
328 macroaggregates (Bach et al., 2018). Our findings support the fact that soil aggregates are distinct
329 habitat spaces with eukaryotes adapted to SOM resources, pore-space network, and water and
330 oxygen availability characteristic of sM and mM.

331

332 *3.3. Effect of conservation management on eukaryotic composition in soil aggregates*

333 To test if conservation tillage and N fertilization shift the composition of soil eukaryotes in soil
334 aggregates (hypothesis 1) and how soil aggregates shape their composition (hypothesis 2), this
335 parameter was evaluated along the soil profile in sM and mM. Across management practices and
336 soil depths, the eukaryotic phyla Cercozoa (21%), Ciliophora (13%), Chlorophyta (11%), Nematoda

337 (11%) and Glomeromycota (9%) were predominant in sM, whereas in mM the predominant phyla
338 were Ciliophora (19%), Cercozoa (18%) Chlorophyta (15%), and Ascomycota (11%) (Fig. 1a). The
339 other phyla showed an abundance ≤ 8%. Sun et al. (2021) found that protists were the most
340 dominant eukaryote (33.9% of the total eukaryotic sequences) in bulk soil. By contrast, Treonis et
341 al. (2018) analysing the whole eukaryotic structure in bulk soil found a high abundance of fungi,
342 Arthropoda, Nematoda and Anellida (40, 20, 20 and 11%, respectively), and a low abundance of
343 protists (0.63%). Among protists, Rhizaria was the group with the highest relative abundance in
344 arable soil, comprising as dominant taxa Cercozoa and Amoebozoa (Bates et al., 2013; Degrune et
345 al., 2019a; Santos et al., 2020). Similarly, in another study, fungi were reported to be the most
346 abundant (i.e., Ascomycota, Basidiomycota, fungi Incertae sedis and Glomeromycota), followed by
347 Alveolata, Metazoa, Rhizaria, Stramenopiles, and Viridiplantae (Chen et al., 2012). Therefore, we
348 can assume that the differences between bulk soil and soil aggregates depend on the variability of
349 pH, moisture and organic nutrient availability that shift soil biota at multiple trophic levels.

350 In both soil aggregates, the majority of taxa were common to all managements across soil
351 depths, whereas some were unique to certain managements, as shown by the Venn diagrams at class
352 resolution (Fig. 2b-c,e-f). This is also shown by the pie charts representing the proportion of the 56
353 classes retrieved in each management (Fig. 2a,d). Moreover, focusing on the shared taxa between
354 sM and mM, ca. 80% of eukaryotes were common to both soil aggregates, averaging soil depths
355 (Fig. 3a,b). Accordingly, a large conserved core community of soil prokaryotes and fungi was
356 found across managements at the same site in bulk soil (Piazza et al., 2019). This is also consistent
357 with the findings obtained in other studies in different soil types and managements in bulk soil as
358 well as in specific rhizocompartments (Lentendu et al., 2014; Edwards et al., 2015; Pershina et al.,
359 2018).

360 However, the exclusive presence of some eukaryotic taxa in the different systems and soil
361 aggregates (Fig. 2) suggests that long-term tillage and N fertilization may drive the development of
362 communities of specialized taxa putatively having specific functions (e.g., soil aggregate and/or

363 SOC accumulation and nutrient cycling). As example, at the surface layer, in sM the classes
364 *Nassophorea* and *Perkinsea* were exclusively found in MTN0, whereas *Pezizomycetes* and
365 *Gastrotricha* in CTN0 (Fig. 2a,b), while many taxa were exclusively found in mM, such as
366 Chlorophyta, *Eutardigrada*, *Eurotiomycetes*, *Nassophorea* and *Thecofilosea* in MTN0; Alveolata,
367 *Chilopoda* and *Rhabditophora* in MTN200 and *Dictyostelia* and *Pezizomycetes* in CTN200 (Fig.
368 2d,e). A more in-depth description of the eukaryotic composition and exclusiveness across
369 managements and aggregates is reported in the Supplementary Results and Discussion 1.
370
371 *3.4. Effect of conservation management on eukaryotic community structures in soil aggregates*

372 To test if conservation tillage and N fertilization shift the structure of soil eukaryotes in soil
373 aggregates (hypothesis 1), the relative abundance pattern of taxa was determined in soil aggregates.
374 Despite the high degree of similarity among treatments in term of community composition, we
375 highlighted a strong effect of the interaction between tillage and N fertilization on the eukaryotic
376 community structures in sM at both soil layers, and in mM only at the surface layer (Table 1, Fig.
377 1). Similarly, soil fungal community structure in bulk soil was strongly shaped by the interaction
378 between tillage and N fertilization at surface and subsurface layers (Piazza et al., 2019). However,
379 to our knowledge no studies have focused on the effect of the interaction of these practices on the
380 eukaryotic communities in soil aggregates, whereas a huge number of studies was performed to
381 assess the effect of tillage or N fertilization on the diversity/abundance and functionality of single
382 eukaryotic group in bulk soil (e.g., fungi: Jansa et al., 2003; Wang et al., 2019; Zhao et al., 2019;
383 micro-arthropods, nematodes and protozoa: Adl et al., 2006; Zhang et al., 2012; Briones and
384 Schmidt, 2017; Cai et al., 2020; protists: Zhao et al., 2019; Sun et al., 2021).

385 In the PCO plots, CTN0 and CTN200 showed similar community structures within sM at
386 surface layer (Fig. 1b) that were characterised by *Colpodea* and OTU1*Spirotrichea* (Ciliophora,
387 Alveolata) and *Conoidasida* (Apicomplexa, Alveolata). This supports that under ploughing N

availability is not limiting and the community structures are not affected by N fertilization. The class *Colpodea* is a well-known dominant clade of mainly bacterivorous protists (Foissner, 1998) and, according to our results, they were shown highly abundant in disturbed soils. By contrast, *Spirotrichea* were found in more stable environments (Lüftenegger et al., 1985), not supporting the large abundance found within sM under ploughed soils. This result not supported by literature may suggest a high resistance of *Spirotrichea* to natural and anthropogenic stresses. Moreover, Apicomplexa that are the third most abundant protistan group in soil, after Cercozoa and Ciliophora (Fierer, 2017) are described as putative parasites of invertebrates (Del Campo et al., 2019). This is in agreement with the lower occurrence of the invertebrates *Chromadorea* and *Enoplea* found in our study under CT compared with MT. In MT, N fertilization determined a strong shift at the surface layer (Fig. 1b), with community structure within sM under MTN200 characterized by a large abundance of taxa belonging to Cercozoa, *Tubulinea* (Lobosa, Amoebozoa) and *Chromadorea* (Nematoda) together with fungi, (i.e., OTU1Microbotryo: *Microbotryomicetes*, Ascomycota and Mortierellomycota), and under MTN0 characterized by a large abundance of taxa belonging to *Imbricatea* (Cercozoa), *Enoplea* (Nematoda) and OTU1*Nassophorea* (Ciliophora, Alveolata). The dominance of Ascomycota in sM under MTN200 is in accordance with their higher abundance in macroaggregates under mineral fertilization compared with no fertilization (Liao et al., 2018; Wang et al., 2021). This confirms the importance of fungi as binding agents in soil aggregates (Six et al., 2000). Cercozoa were reported to be affected by several abiotic factors, as soil moisture, clay content and N availability (Lentendu et al., 2014; Fiore-Donno et al., 2019). However, although our analyses did not allow discrimination of which cercozoan classes were favoured under MTN200 (Fig. 1b), the detection of *Imbricatea* within sM under MTN0 supports that N availability is a major driver of cercozoan communities. This class had unexpectedly high abundance in sM under MTN0 (Fig. 1b), although it was shown to be highly favoured by organic fertilizers (Lentendu et al., 2014). According to our results (Fig. 1b), the heterotroph lineage Tubulinea are dominant in highly N-fertilizer soils (Sun et al., 2021), and the ciliate *Nassophorea*, characterizing the community

414 structures of sM under MTN0, supports their role in energy transfer between trophic levels under
415 low N availability (Gao et al., 2016). Finally, the dominance in sM under MT of *Enoplea* and
416 *Chromadorea* known to be plant and animal nematode parasites is consistent with their general
417 trend in soil aggregates (Jiang et al., 2017). Their abundance in N0 and N200, respectively, might
418 be explained by specific predator-prey interactions occurring within intra-aggregate pores at
419 differential N availabilities.

420 At the subsurface layer (Fig. 1c), N fertilization drove a stronger shift of the eukaryotic
421 community structure in sM under CT compared with MT that showed similar structures irrespective
422 to N fertilization, highlighting an opposite pattern as compared with the one observed at surface
423 layer (Fig. 1b). Under CTN0, sM was characterised by high abundance of *Chilopoda* (Arthropoda,
424 Animalia) and *Sarcomonadea* (Cercozoa, Rhizaria), and under CTN200 by high abundance of
425 *Colpodea* and *Conoidasida* (Alveolata) (Fig. 1c). Indeed, under ploughing, the subsurface layer is
426 less compacted than under MT and shows a lower bulk density, resulting in an increase of pore size
427 and aeration (Berisso et al., 2012). This may allow a larger root development under N fertilization
428 and a higher variation in soil moisture and temperature compared with no fertilization (Piazza et al.,
429 2020). Small macroaggregates are inaccessible to living centipedes (*Chilopoda*), thus their
430 abundance in this fraction under CTN0 can be only related to a role as binding agents or as dead
431 biomass consumed by decomposers. By contrast, *Sarcomonadea*, previously found in soil as the
432 dominant class within the phylum Cercozoa (Degrune et al., 2019b), are likely to play an active role
433 also in sM at low N availabilities. The abundance of *Colpodea* in CTN200 at the subsurface layer
434 (Fig. 1c) is consistent with their dominance at the surface layer (Fig. 1b) and can be explained by
435 bacterial pray changes following N application, while no information is available on *Conoidasida*
436 trophic functional role.

437 In MTN0 and MTN200 at subsurface layer sM were characterized by *Chromadorea*
438 (Nematoda), *Vampyrellidea* (Cercozoa), OTU1*Nassophorea* (Ciliophora, Alveolata) and many
439 fungi (e.g., *Glomeromycetes*, *Sordariomycetes*) (Fig. 1c). The abundance of *Choromadorea* and

440 *Nassophorea* is consistent with surface layer observations. Moreover, *Vampyrellidea,* observed for
441 the first time in sM, are fungivores that may control the parasitic rust fungus of wheat under MT
442 (Adl and Gupta, 2006). Finally, the abundance of *Glomeromycetes* and *Sordariomycetes* confirms
443 their crucial role in driving soil aggregates under undisturbed conditions (Rillig et al., 2015; Wang
444 et al., 2021).

445 In mM, a strong interaction effect between tillage and N fertilization was found on the
446 eukaryotic community structures only at surface layer, consisting in a strong shift of the structure
447 under CTN0 compared with the other treatments (Table 1, Fig. 1d). This effect is in line with the
448 aggregate distribution of mM found by Piazza et al. (2020). The shifts of aggregate distribution and
449 eukaryotic community structure toward more mM and distinct soil biota communities under CT at
450 low N availability can be related to a lower sequestration of C within mM and thus in differences of
451 the related functional soil biota. By contrast, the lack of effect at subsurface layer is unexpected
452 since the percentage of mM was significantly decreased by tillage intensification (CT < MT; - 21%)
453 (Piazza et al., 2020). However, this inconsistency could be due to the coverage of the V4 region
454 primer set, its taxonomic resolution or limitation in amplifying rare taxa or taxa with lower
455 proportions of template DNA in DNA extracts (Choi and Park, 2020). Moreover, considering
456 aggregate pore size and animal body size, the presence of traces of animal DNA (i.e., nematodes,
457 Arthropoda) within aggregates is likely not attributable to the occurrence of living animals, but to
458 the process of aggregate formation which utilises organic decaying material as binding agent.

459 Nitrogen fertilization determined a strong shift at the surface layer in the eukaryotic community
460 structure of mM under CT (Fig. 1d) from *Glomeromycetes* (Glomeromycota), *Imbricatea*,
461 *Sarcomonadea* and *Vampyrellidea* (Cercozoa) in CTN0 to OTU1*Xantho* (Ochrophyta),
462 *Oligohymenophorea* (Ciliophora), Stramenopiles (Chromista) and the fungus *Tremellomycetes* in
463 CTN200. This is the first time that Glomeromycota have been detected within mM fraction.
464 Previously, using a cloning approach targeting the long-fragment SSU-ITS-LSU (Krüger et al.,
465 2009) we could not detect AMF within mM (data not shown), and this was also supported by

several works reporting their major roles only in macroaggregates (e.g., Miller and Jastrow, 2000, Rillig et al., 2002). However, in this study, the observed large proportion of Glomeromycota (14%) in mM under CTN0 supports the fact that tillage under unfertilized conditions may not negatively affect the development of the extraradical mycelium, potentially improving the production of glomalin and enhancing soil aggregate stability (Bedini et al., 2002). Similarly, the high abundance of Cercozoa in mM under CTN0 suggests for the first time that this phylum plays a major role within mM under ploughed and no fertilized conditions at surface layer. This is consistent with the findings of Degrune et al. (2019a) that highlighted under ploughing and at topsoil distinct cercozoan communities in microhabitats (i.e., drilosphere and rhizosphere) compared with bulk soil. Moreover, the distinct eukaryotic community found at surface layer in mM under CTN200 additionally supports that, under ploughing, nutrient availabilities in microhabitats allow the dominance of functional protists (Alveolata: *Oligohymenophorea*; Chromista: OTU1*Xantho* and Stramenopiles), potentially contributing to OM decomposition and mineralization through several functional groups. In addition, scarce information is available on the functional roles in agricultural soils of *Tremellomycetes*, a heterogeneous group comprising saprotrophs, animal parasites, and fungicolous species.

Similar community structures were observed at surface layer within mM in MTN0 and MTN200 [e.g., *Sarcomonadea*1 (Cercozoa), and fungi such as *Dothideomycetes* (Ascomycota) and OTU1Cystobasidio (Basidiomycota)] (Fig. 1d). These results support the hypothesis of a major role played by Cercozoa together with distinct classes of fungi also within mM under MT. However, it is well known that the 18S barcoding utilised in this work is less efficient compared with the ITS for detecting many groups of fungi (Schoch et al., 2012).

To test if soil aggregates differentially shape the structure of soil eukaryotes (hypothesis 2), the relative abundance pattern of taxa was determined in sM and mM. Significant differences among matrices (sM *vs* mM) were found and supported by PERMANOVAs (Table 1). PCO biplots showed that at both soil layers more phyla were linked to mM as compared with sM (Fig. 3c,d).

Recently, Liao et al. (2018) and Wang et al. (2021) used an Illumina sequencing approach for studying at phylum and class level the bacterial and fungal community structures within soil aggregates across different fertilization treatments. Although differences in community structure were detected for both bacteria and fungi, fungal community in sM and free microaggregates differed more than bacteria (Liao et al., 2018; Wang et al., 2021). Our findings support that some unresolved taxa belonging to Glomeromycota and Ascomycota are positively associated with mM, as previously reported in free microaggregates for unclassified Ascomycota (Wang et al., 2021) and for a group of unclassified *Glomerales* (Lu et al., 2018). Similarly to the results of Jiang et al. (2017), the total abundance of nematodes increased with increasing aggregate size. Finally, the alveolate Apicomplexa, Ciliophora, and Dinoflagellata were preferentially found in mM, whereas the amoebozoan Conosa and Lobosa in sM. This result additionally confirms the functional role played by protists within microenvironments. Moreover, Mollusca in mM and Arthropoda and Anellida in sM at both soil layers can be considered as preferential binding agents for aggregate fractions.

*Eukaryotic taxa predictors for soil structuring and C stocks*

To test if some eukaryotic taxa are predictors for soil structuring and C stock (hypothesis 3) we utilised a multiple regression analysis that allowed to identify the eukaryotic taxa that were good predictors for the amount of sM and mM and their SOC content, irrespective of management and soil depth (Table S1). Specifically, *Microbotryomycetes* and Alveolata were moderately strongly related to the amount of sM, with *Microbotryomycetes* identified as best predictor. Similarly, Cercozoa and *Chytridiomycetes* were related to the amount of mM, with Cercozoa playing the major role. Moreover, *Microbotryomycetes*, Cercozoa and Alevolata were moderately related to SOC in sM, with *Microbotryomycetes* consistently found to be the best predictor. Finally, *Chytridiomycetes* and Cercozoa were moderately related to SOC in mM, with *Chytridiomycetes* the best predictor. Previously, Bach et al. (2018) identified bacterial and fungal indicators in free and

large macroaggregates. However, it is the first time that *Microbotryomycetes* and *Chytridiomycetes* have been shown to be correlated with the amount of sM and mM and their SOC content, respectively. Both fungal classes correlated with the pattern of C-cycling enzymes and SOC content in bulk soil (Piazza et al., 2019), and their abundance was high in sM and mM, respectively (Degrune et al., 2019b). *Microbotryomycetes* were also recently identified as good predictors of slow and passive SOC decomposition parameters (Hale et al., 2019). Our findings on the positive association of protists, Alveolata and Cercozoa, with the amount of sM and mM and their SOC content, support the multiple agroecological roles of protists found in bulk soil (Cavalier-Smith and Chao, 2003; Delgado-Baquerizo et al., 2020). Moreover, our results confirm previous works reporting that protists are shaped by pore size reduction and soil aeration (Berisso et al., 2012; Degrune et al., 2019a), features related to soil aggregates. Thus, we can assume that Alveolata are playing major role in soil, promoting sM formation and slowing down the decay of SOM within sM, while Cercozoa are crucial microorganisms in mM taking part to long-term sequestration and storing of SOC.

### *3.6. How eukaryotes are interlinked among each other and to prokaryotes in soil aggregates, and network traits predictor for soil structuring and C stocks*

To test if eukaryotes form structured assemblages and distinctive networks in soil aggregates (hypothesis 4), and how eukaryotes are linked to prokaryotes (hypothesis 5), within- and cross-domain networks were built for sM and mM. At the surface layer within- and cross-domain networks were more complex in mM than in sM, whereas at the subsurface layer they did not vary (Table 2, Fig. 4, Fig. S6). In the cross-domain networks, both sM and mM showed a general trend toward a higher percentage of eukaryotes per subnetwork compared to prokaryotes at the surface layer compared with the subsurface layer (Table 3, Fig. 4b,d). Moreover, at both soil depth, in the sM cross-domain networks the majority of subnetworks were composed of both eukaryotes and

prokaryotes, whereas in the mM cross-domain networks the subnetworks were half composed of eukaryotes and half of prokaryotes, and few subnetworks were mixed (Table 3). This is the first study that demonstrated that eukaryotes, components of soil biota communities usually studied separately, formed structured associations within each other and with prokaryotes in soil aggregates. Moreover, mM consistently had tighter connectivity compared with sM in both within- and cross-domain networks (Fig. 4, Fig. S6). This might be related to microhabitat conditions (i.e., wetter and more nutrient rich microhabitats) in mM that shift biotic interactions from facilitation to competition, leading to higher correlations between eukaryotic taxa or eukaryotic and prokaryotic taxa, as previously reported for fungi and bacteria in bulk soil and roots across land uses and agricultural managements with a gradient of nutrient availabilities (e.g., SOC, P levels) and pH (de Menezes et al., 2015; Banerjee et al., 2016, 2018; Wang et al., 2021). Other explanations could be a higher proportion of viable cells and spores and a lower niche heterogeneity (i.e., nutrients) in mM respect to sM, leading to tighter within- and cross-domain networks. Finally, a higher plant residue diversity in mM could also explain the within- and cross-domain mM network traits, as previously shown for plant community composition or host selectivity against microbial network complexity (Xiong et al., 2021).

In the within-domain networks of sM and mM and at both soil layers, Cercozoa were highly co-occurring in the subnetworks respect to the other eukaryotic phyla, as shown by the network traits (Table 3, Supplementary Results and Discussions 2). It is noteworthy the high percentage of taxa belonging to Cercozoa (21%) involved in the largest subnetworks, composed of 33, occurring at surface layer in the within-domain mM networks. In addition, while fungi, mainly Ascomycota and Basidiomycota, were highly co-occurring in the within-domain sM subnetworks at both soil layer, protists, as Ochrophyta and Stramenopiles together with Chlorophyta, were co-occurring in the within-domain mM subnetworks at surface and subsurface layer, respectively (Table 2). Following the definition of keystone taxa by Banerjee et al. (2018), we can support the agroecological theory that some Cercozoa, as *Sarcomondea* and *Vampyrillidea* (Fig. 4c), can be

569 suggested as “hubs” (keystone taxa) within mM. Consistently, in the sM and mM cross-domain
570 networks at the surface layer, Cercozoa can be considered as “hubs” as they are directly connected
571 to prokaryotes in the largest subnetworks (Fig. 4b,d). Moreover, protists were involved in the
572 largest subnetworks and showed variable direct connections (Fig. 4b,d, Fig. S6b,d). Indeed, the
573 linkages of protists, according to their feeding versatility (Geisen, 2016), varied from direct
574 connections to many prokaryotes, mainly belonging to Chloroflexi in the cross-domain sM
575 networks (Fig. 4b, Fig. S6b), to direct linkages to other eukaryotes (e.g., fungi) or other protists in
576 mM networks (Fig. 4d, Fig. S6d). So far, studies on the functional roles of soil biota in the
577 formation of soil aggregates have mainly focused on the role played by a single functional group,
578 e.g. AMF, earthworms, nematodes, termites and microarthropods (mites and collembolans) (e.g.,
579 Lee and Foster, 1991; Pulleman et al., 2005; Rillig and Mummey, 2006; Siddiky et al., 2012a,b;
580 Zhang et al., 2016). However, only recently, Cercozoa and other protists, as Lobosa and Ciliophora,
581 were shown to be positively related with ecosystem services, i.e. nutrient cycling and OM
582 decomposition (Delgado-Baquerizo et al., 2020). Details about traits and taxa co-occurrences in
583 within- and cross-domain networks and the significance of cross-domain relationships (Mantel test
584 and CoCA) are given in Supplementary Results and Discussion 2, Fig. S7 and Fig. S8.

585 To test if some network traits can predict soil structuring and C stocks, we utilized a multiple
586 regressions analysis that identified the number of edges and mean nodes per network as predictors
587 for the amount of sM and mM and their SOC content, irrespective of management and soil depth
588 (Table S2). Although network analysis is now largely applied to study soil biota co-occurrence and
589 plant-microbe associations across different treatments (e.g., de Menezes et al., 2015; Farrer et al.,
590 2019; Feng et al., 2019), little is known about soil biota networks within aggregates (Jiang et al.,
591 2015, 2017) and few studies have dissected the predictable power of the network traits (topological
592 properties) on ecosystem services. Jiang et al. (2015, 2017) indicated that aggregate fractions (large
593 and small macroaggregates, and free microaggregates) showed a strong effect on the association
594 networks of nematodes and bacteria and using the topological properties they could identify large

595 macroaggregates network as organized soil food web, showing functional interrelationships
596 between bacterivorous nematodes and bacteria. In accordance with our results, the topological
597 properties of soil biota networks should be taken into consideration for dissecting soil structuring as
598 well as C cycling.
599

600 **4. Conclusions**

601 We have shown that soil aggregation is essential for a complete 'multifunctional' perspective
602 of soil biota. A full understanding of relationships between soil biota and soil functions requires
603 analyses emphasizing the feedbacks between soil structure and soil biota, rather than a
604 unidirectional approach simply addressing the roles of single key functional groups. Next
605 generation sequencing tools have been confirmed in this study to be crucial in the understanding of
606 eukaryotic structures and soil biota networks and have the potential to further reveal their
607 contributions to soil functions. Indeed, our findings demonstrate for the first time that protists
608 together with fungi play major roles in soil structuring and C cycling, and that Cercozoa represent
609 hubs in the soil biota aggregate networks. This supports the fact that their conservation is
610 fundamental to prevent soil degradation and to enhance SOC accumulation in agroecosystems.
611

612 **Declaration of competing interest**

613 The authors declare that they have no known competing financial interests or personal
614 relationships that could have appeared to influence the work reported in this paper.
615

616 **Acknowledgments**

617 This work was funded by the European Agricultural Fund for Rural Development 2007-2013
618 for Tuscany (Italy), measure 16.1 and 16.2 for GO groups (FERTIBIO project) (CUP Artea 743548
619 and CUP Artea 828090), project leader Dr. Elisa Pellegrino. Dr. Gaia Piazza was supported by a

PhD scholarship and a further postdoc fellowship at the Scuola Superiore Sant'Anna (Pisa, Italy). Thorunn Helgason was supported by UKRI-NERC grants NE/M004864/1 & NE/M017095/1. We acknowledge the contribution of Dr Joe Taylor who provided protocols and support to Dr Piazza. A special thanks to our mentor Emeritus Prof. Marco Nuti University of Pisa (Professor affiliate to the Institute of Life Sciences, Scuola Superiore Sant'Anna) for advice during the discussion of results and proof reading of the paper.

## References

Adl, M.S., Gupta, V.S., 2006. Protists in soil ecology and forest nutrient cycling. Canadian Journal of Forest Research 36, 1805–1817.

Adl, M.S., Coleman, D.C., Read, F., 2006. Slow recovery of soil biodiversity in sandy loam soils of Georgia after 25 years of no-tillage management. Agriculture, Ecosystem and Environment 114, 323–334.

Anderson, M., Braak, C.T., 2003. Permutation tests for multi-factorial analysis of variance. Journal of Statistical Computation and Simulation 73, 85–113.

Anderson, M.J., Gorley, R.N., Clarke, R.K., 2008. Permanova+ for Primer: Guide to Software and Statistical Methods. Primer-E Limited.

Aune, J. B., 2012. Conventional, organic and conservation agriculture: production and environmental impact. In: Lichtfouse E. (Eds), Agroecology and strategies for climate change. Sustainable Agriculture Reviews, vol 8. Springer: Dordrecht, NL, pp. 149–165.

Bach, E.M., Williams, R.J., Hargreaves, S.K., Yang, F., Hofmockel, K.S., 2018. Greatest soil microbial diversity found in micro-habitats. Soil Biology and Biochemistry 118, 217–226.

Banerjee, S., Baah-Acheamfour, M., Carlyle, C.N., Bissett, A., Richardson, A.E., Siddique, T., Bork, E.W., Chang, S.X., 2016. Co-occurrence patterns of soil bacterial communities. Environmental Microbiology 18, 1805–1816.

645 Banerjee, S., Schlaeppi, K., van der Heijden, M.G., 2018. Keystone taxa as drivers of microbiome
646 structure and functioning. Nature Reviews Microbiology 16, 567–576.
647 Bates, S.T., Clemente, J.C., Flores, G.E., Walters, W.A., Parfrey, L.W., Knight, R., et al., 2013.
648 Global biogeography of highly diverse protistan communities in soil. The ISME Journal 7, 652.
649 Bedini, S., Pellegrino, E., Avio, L., Pellegrini, S., Bazzoffi P, Argese E, Giovannetti, M., 2009.
650 Changes in soil aggregation and glomalin-related soil protein content as affected by the
651 arbuscular mycorrhizal fungal species *Glomus mosseae* and *Glomus intraradices*. Soil Biology
652 and Biochemistry 41, 1491–1496.
653 Berisso, F. E., Schjønning, P., Keller, T., Lamandé, M., Etana, A., de Jonge, L.W., Iversen, B.V.,
654 Arvidsson, J., Forkmann, J., 2012. Persistent effects of subsoil compaction on pore size
655 distribution and gas transport in a loamy soil. Soil and Tillage Research 122, 42–51.
656 Bossuyt, H., Six, J., Hendrix, P.F, 2006. Interactive effects of functionally different earthworm
657 species on aggregation and incorporation and decomposition of newly added residue carbon.
658 Geoderma 130, 14–25.
659 Bremner, J.M., Mulvaney, C.S., 1982. Nitrogen - total 1. Methods of soil analysis. Part 2. Chem.
660 Microbiol. Properties, pp. 595-624.
661 Briones, M.J.I., Schmidt, O., 2017. Conventional tillage decreases the abundance and biomass of
662 earthworms and alters their community structure in a global meta-analysis. Global Change
663 Biology 23, 4396–4419.
664 Cai, S., Wang, J., Lv, W., Xu, S., Zhu, H., 2020. Nitrogen fertilization alters the effects of
665 earthworms on soil physicochemical properties and bacterial community structure. Applied
666 Soil Ecology 150, 103478.
667 Caporaso, J.G., Lauber, C.L., Walters, W.A., Berg-Lyons, D., Huntley, J., Fierer, N., et al, 2012.
668 Ultra-high-throughput microbial community analysis on the Illumina HiSeq and MiSeq
669 platforms. The ISME Journal 6, 1621.

670 Cavalier-Smith, T., Chao, E.E.Y., 2003. Phylogeny and classification of phylum Cercozoa
671 (Protozoa). Protist 154, 341–358.
672 Chen, M., Li, X., Yang, Q., Chi, X., Pan, L., Chen, N., et al., 2012. Soil eukaryotic microorganism
673 succession as affected by continuous cropping of peanut-pathogenic and beneficial fungi were
674 selected. Plos One 7, e40659.
675 Choi, J., Park, J.S., 2020. Comparative analyses of the V4 and V9 regions of 18S rDNA for the
676 extant eukaryotic community using the Illumina platform. Scientific Report 10, 1–11.
677 Clarke, K.R., Gorley, R.N., 2006. PRIMER v6: User Manual/Tutorial. PRIMER-E: Plymouth, UK.
678 de Menezes, A.B., Prendergast- Miller, M.T., Richardson, A.E., Toscas, P., Farrell, M.,
679 Macdonald, L.M., Baker, G., Wark, T. and Thrall, P.H., 2015. Network analysis reveals that
680 bacteria and fungi form modules that correlate independently with soil
681 parameters. Environmental Microbiology 17, 2677–2689.
682 De Vries, F.T., Thébault, E., Liiri, M., Birkhofer, K., Tsiafouli, M.A., Bjørnlund, L., Bracht
683 Jørgensen, H., Brady, M.V., Christensen, S., de Ruiter, P.C., d'Hertefeldt, T., Frouz, J.,
684 Hedlund, K., Hemerik, L., Hol, W.H.G., Hotes, S., Mortimer, S.R., Setälä, H., Sgardelis, S.P.,
685 Uteseny, K., W.H., Wolters, V., Bardge, R.D., 2013. Soil food web properties explain
686 ecosystem services across European land use systems. Proceedings of the National Academy of
687 Sciences 110, 14296–14301.
688 Degrune, F., Boeraeve, F., Dufrêne, M., Cornélis, J.T., Frey, B., Hartmann, M., 2019a. The
689 pedological context modulates the response of soil microbial communities to agroecological
690 management. Frontiers in Ecology and Evolution 7, 261.
691 Degrune, F., Dumack, K., Fiore-Donno, A.M., Bonkowski, M., Sosa-Hernández, M.A., Schloter,
692 M., Kautz, T., Fischer, D., Rillig, M.C., 2019b. Distinct communities of Cercozoa at different
693 soil depths in a temperate agricultural field. FEMS Microbiology Ecology 95, fiz041.
694 Del Campo, J., Heger, T.J., Rodríguez-Martínez, R., Worden, A.Z., Richards, T.A., Massana, R.,
695 Keeling, P.J., 2020. Assessing the diversity and distribution of apicomplexans in host and free-

696 living environments using high-throughput amplicon data and a phylogenetically informed
697 reference framework. Frontiers in Microbiology 10, 2373.
698 Delgado-Baquerizo, M., Reich, P.B., Trivedi, C., Eldridge, D.J., Abades, S., Alfaro, F.D., Bastida,
699 F., Berhe, A.A., Cutler, N.A., Gallardo, A., García-Velázquez, L., Hart, S.C., Hayes, P.E., He,
700 J., Hseu,Z., Hu, H., Kirchmair, M., Neuhauser, S., Pérez, C.A., Reed, S.C., Santos, F., Sullivan,
701 B.W., Trivedi, P., Wang, J., Weber-Grullon, L., Williams M.A., Singh, B.K., 2020. Multiple
702 elements of soil biodiversity drive ecosystem functions across biomes. Nature Ecology and
703 Evolution 4, 210–220.
704 Denef, K., Zotarelli, L., Boddey, R.M., Six, J., 2007. Microaggregate-associated carbon as a
705 diagnostic fraction for management-induced changes in soil organic carbon in two Oxisols. Soil
706 Biology and Biochemistry 39, 1165–1172.
707 Duan, Y., Chen, L., Zhang, J., Li, D., Han, X., Zhu, B., Li, Y., Zhao, B., Huang, P., 2021. Long-
708 term fertilisation reveals close associations between soil organic carbon composition and
709 microbial traits at aggregate scales. Agriculture, Ecosystem and Environment 306, 107169.
710 Edgar, R.C., 2010. Search and clustering orders of magnitude faster than BLAST. Bioinformatics
711 26, 2460-2461.
712 Edgar, R.C., Flyvbjerg, H., 2015. Error filtering, pair assembly and error correction for next
713 generation sequencing reads. Bioinformatics 31, 3476-3482.
714 Edwards, J., Johnson, C., Santos-Medellín, C., Lurie, E., Podishetty, N.K., Bhatnagar, S., Eisen,
715 J.A., Sundaresan, V., 2015. Structure, variation, and assembly of the root-associated
716 microbiomes of rice. Proceedings of the National Academy of Sciences 112, E911–E920.
717 Elliott, E.T., 1986. Aggregate structure and carbon, nitrogen, and phosphorus in native and
718 cultivated soils. Soil Science Society of America Journal 50, 627–633.
719 Ercoli, L., Schüßler, A., Arduini, I., Pellegrino, E., 2017. Strong increase of durum wheat iron and
720 zinc content by field-inoculation with arbuscular mycorrhizal fungi at different soil nitrogen
721 availabilities. Plant and Soil 419, 153–167.

722 Farrer, E.C., Porazinska, D.L., Spasojevic, M.J., King, A.J., Bueno de Mesquita, C.P., Sartwell,
723 S.A., Smith, J.G., White, C.T., Schmidt, S.K., Suding, K.N., 2019. Soil microbial networks
724 shift across a high-elevation successional gradient. Frontiers in Microbiology 10, 2887.
725 Feng, K., Zhang, Y., He, Z., Ning, D., Deng, Y., 2019. Interdomain ecological networks between
726 plants and microbes. Molecular Ecology Resources 19, 1565–1577.
727 Fierer, N., 2017. Embracing the unknown: disentangling the complexities of the soil microbiome.
728 Nature Reviews Microbiology 15, 579–590.
729 Fiore-Donno, A.M., Richter-Heitmann, T., Degrune, F., Dumack, K., Regan, K.M., Marhan, S.,
730 Boeddinghaus, R.S., Rillig, M.C., Friedrich, M.W., Kandeler, E., Bonkowski, M., 2019.
731 Functional traits and spatio-temporal structure of a major group of soil protists (Rhizaria:
732 Cercozoa) in a temperate grassland. Frontiers in Microbiology 10, 1332.
733 Foissner, W., 1998. An updated compilation of world soil ciliates (protozoa, Ciliophora), with
734 ecological notes, new records, and descriptions of new species. European Journal of
735 Protistology 34, 195–235.
736 Fonte, S.J., Kong, A.Y., van Kessel, C., Hendrix, P.F., Six, J., 2007. Influence of earthworm
737 activity on aggregate-associated carbon and nitrogen dynamics differs with agroecosystem
738 management. Soil Biology and Biochemistry 39, 1014–1022.
739 Franzluebbers, A.J., Arshad, M.A., 1997. Particulate organic carbon content and potential
740 mineralization as affected by tillage and texture. Soil Science Society of America Journal 61,
741 1382–1386.
742 Gao, F., Warren, A., Zhang, Q., Gong, J., Miao, M., Sun, P., Xu, D., Huang, J., Yi, Z., Song, W.,
743 2016. The all-data-based evolutionary hypothesis of ciliated protists with a revised
744 classification of the phylum Ciliophora (Eukaryota, Alveolata). Scientific Report 6, 24874.
745 Geisen, S., 2016. The bacterial-fungal energy channel concept challenged by enormous functional
746 versatility of soil protists. Soil Biology and Biochemistry 102, 22–25.

747 Ghosh, A., Bhattacharyya, R., Dey, A., Dwivedi, B. S., Meena, M. C., Manna, M. C., Agnihortri, R.
748 2019. Long-term fertilisation impact on temperature sensitivity of aggregate associated soil
749 organic carbon in a sub-tropical inceptisol. Soil and Tillage Research 195, 104369.
750 Gloor, G. B., Macklaim, J. M., Pawlowsky-Glahn, V., Egozcue, J. J. 2017. Microbiome datasets are
751 compositional: and this is not optional. Frontiers in Microbiology 8, 2224.
752 Grandin, U., 2006. PC-ORD version 5: a user-friendly toolbox for ecologists. Journal of Vegetation
753 Science 17, 843–844.
754 Guan, D., Al-Kaisi, M. M., Zhang, Y., Duan, L., Tan, W., Zhang, M., Li, Z., 2014. Tillage practices
755 affect biomass and grain yield through regulating root growth, root-bleeding sap and nutrients
756 uptake in summer maize. Field Crops Research 157, 89-97.
757 Gupta, V.V., Germida, J.J., 2015. Soil aggregation: Influence on microbial biomass and
758 implications for biological processes. Soil Biology and Biochemistry 80, A3–A9.
759 Hale, L., Feng, W., Yin, H., Guo, X., Zhou, X., Bracho, R., Pegoraro, E., Penton, C.R., Wu, L.,
760 Cole, J., Konstantinidis, K.T., Luo, Y., Tiedje, J.M., Schuur, E.A.G., Zhou, J., 2019. Tundra
761 microbial community taxa and traits predict decomposition parameters of stable, old soil
762 organic carbon. The ISME Journal 2019 13, 2901–2915.
763 Heberle, H., Meirelles, G.V., da Silva, F.R., Telles, G.P., Minghim, R., 2015. InteractiVenn: a web-
764 based tool for the analysis of sets through Venn diagrams. BMC Bioinformatics 16, 169.
765 Himmelstein, J., Ares, A., Gallagher, D., Myers, J., 2016. A meta-analysis of intercropping in
766 Africa: impacts on crop yield, farmer income, and integrated pest management effects.
767 International Journal of Agricultural Sustainability 15, 1–10.
768 IUSS working group WRB., 2006. World reference base for soil resources 2006 - A framework for
769 international classification, correlation and communication. Food and Agriculture Organization
770 of the United Nations: Rome, Italy.

771 Jansa, J., Mozafar, A., Kuhn, G., Anken, T., Ruh, R., Sanders, I.R., Frossard, E.J.E.A., 2003. Soil
772 tillage affects the community structure of mycorrhizal fungi in maize roots. Ecological
773 Applications 13, 1164–1176.
774 Jastrow, J.D., Miller, R.M., 1998. Soil aggregate stabilization and carbon sequestration: feedbacks
775 through organomineral associations. In: Lal, R., Kimble, J.M., Follett, R.F., Stewart, B.A.
776 (Eds). Soil processes and the carbon cycle. CRC Press, New York, USA, pp. 207–223.
777 Jiang, Y., Liu, M., Zhang, J., Chen, Y., Chen, X., Chen, L., Li, H., Zhang X., Sun, B., 2017.
778 Nematode grazing promotes bacterial community dynamics in soil at the aggregate level. The
779 ISME Journal 11, 2705–2717.
780 Jiang, Y., Sun, B., Li, H., Liu, M., Chen, L., Zhou, S., 2015. Aggregate-related changes in network
781 patterns of nematodes and ammonia oxidizers in an acidic soil. Soil Biology and Biochemistry
782 88, 101–109.
783 Kong, A.Y., Scow, K.M., Córdova-Kreylos, A.L., Holmes, W.E., Six, J., 2011. Microbial
784 community composition and carbon cycling within soil microenvironments of conventional,
785 low-input, and organic cropping systems. Soil Biology and Biochemistry 43, 20–30.
786 Kottek, M., Grieser, J., Beck, C., Rudolf, B., Rubel, F., 2006. World map of the Köppen-Geiger
787 climate classification updated. Meteorologische Zeitschrift 15, 259–263.
788 Krüger, M., Stockinger, H., Krüger, C., Schüßler, A., 2009. DNA- based species level detection of
789 Glomeromycota: one PCR primer set for all arbuscular mycorrhizal fungi. New Phytologist
790 183, 212–223.
791 Kumar, S., Stecher, G., Tamura, K., 2016. MEGA7: molecular evolutionary genetics analysis
792 version 7.0 for bigger datasets. Molecular Biology and Evolution 33, 1870-1874.
793 Kurtz, Z.D., Müller, C.L., Miraldi, E.R., Littman, D.R., Blaser, M.J., Bonneau, R.A., 2015. Sparse
794 and compositionally robust inference of microbial ecological networks. PLoS Computational
795 Biology 11, e1004226.

796 Lagomarsino, A., Grego, S., Kandeler, E., 2012. Soil organic carbon distribution drives microbial
797 activity and functional diversity in particle and aggregate-size fractions. Pedobiologia 55, 101–
798 110.
799 Lal, R., Negassa, W., Lorenz, K., 2015. Carbon sequestration in soil. Current Opinion in
800 Environmental Sustainability 15, 79–86.
801 Lee, K.E., Foster, R.C., 1991. Soil fauna and soil structure. Soil Research 29, 745–775.
802 Lehmann, A., Zheng, W., Rillig, M.C., 2017. Soil biota contributions to soil aggregation. Nature
803 Ecology and Evolution 1, 1828.
804 Lentendu, G., Wubet, T., Chatzinotas, A., Wilhelm, C., Buscot, F., Schlegel, M., 2014. Effects of
805 long-term differential fertilization on eukaryotic microbial communities in an arable soil: a
806 multiple barcoding approach. Molecular Ecology 23, 3341–3355.
807 Liao, H., Zhang, Y., Zuo, Q., Du, B., Chen, W., Wei, D., Huang, Q., 2018. Contrasting responses of
808 bacterial and fungal communities to aggregate-size fractions and long-term fertilizations in
809 soils of northeastern China. Science of the Total Environment 635, 784–792.
810 Liu, H., Roeder, K., Wasserman, L., 2010. Stability Approach to Regularization Selection (StARS)
811 for High Dimensional Graphical Models. Advances in Neural Information Processing Systems
812 24, 1432–40.
813 Lu, X., Lu, X., Liao, Y., 2018. Effect of tillage treatment on the diversity of soil arbuscular
814 mycorrhizal fungal and soil aggregate-associated carbon content. Frontiers in Microbiology 9,
815 2986.
816 Lüftenegger, G., Foissner, W., Adam, H., 1985. R- and K-selection in soil ciliates: a field and
817 experimental approach. Oecologia 66, 574–579.
818 Mantel, N., Valand, R.S., 1970. A technique of nonparametric multi-variate analysis. Biometrics
819 26, 547–558.
820 Meinshausen, N., Bühlmann, P., 2010. Stability selection. Journal of the Royal Statistical Society
821 Series B (Statistical Methodology) 72, 417–473.

822 Miller, R.M., Jastrow, J.D., 2000. Mycorrhizal fungi influence soil structure. In: Kapulnik, Y.,
823 Douds, D.D. (Eds). Arbuscular mycorrhizas: physiology and function. Springer, Dordrecht,
824 ND, pp. 3–18.
825 Morriën, E., Hannula, S.E., Snoek, L.B., Helmsing, N.R., Zweers, H., De Hollander, M., Soto, R.L.,
826 Bouffaud, M., Buée, M., Dimmers, W., Duyts, H., Geisen, S., Girlanda, M., Griffiths, R.I.,
827 Jørgensen, H., Jensen, J., Plassart, P., Redecker, D., Schmelz, R.M., Schmidt, O., Thomson,
828 B.C., Tisserant, E., Uroz, S., Winding, A., Bailey, M.J., Bonkowski, M., Faber, J. H., Martin,
829 F., Lemanceau, P., de Boer, W., van Veen J.A., van der Putten, W.H., 2017. Soil networks
830 become more connected and take up more carbon as nature restoration progresses. Nature
831 Communication 8, 1–10.
832 Oksanen, J., Blanchet, F.G., Kindt, R., Legendre, P., Minchin, P.R., O'hara, R.B., et al., 2013.
833 Package 'vegan'. Community Ecology Package, version 2.9.
834 Onweremadu, E.U., Onyia, V.N., Anikwe, M.A.N., 2007. Carbon and nitrogen distribution in
835 water-stable aggregates under two tillage techniques in Fluvisols of Owerri area, southeastern
836 Nigeria. Soil and Tillage Research 97, 195–206.
837 Pershina, E.V., Ivanova, E.A., Korvigo, I.O., Chirak, E.L., Sergaliev, N.H., Abakumov, E.V.,
838 Provorov, N.A., Andronov, E.A., 2018. Investigation of the core microbiome in main soil types
839 from the East European plain. Science of the Total Environment 631, 1421–1430.
840 Piazza, G., 2019. Soil carbon and microbial diversity under conservation management practices.
841 Doctoral dissertation, Scuola Superiore Sant'Anna, Pisa, Italy.
842 Piazza, G., Ercoli, L., Nuti, M., Pellegrino, E., 2019. Interaction between conservation tillage and
843 nitrogen fertilization shapes prokaryotic and fungal diversity at different soil depths: evidence
844 from a 23-year field experiment in the Mediterranean area. Frontiers in Microbiology 10, 2047.
845 Piazza, G., Pellegrino, E., Moscatelli, M.C., Ercoli, E., 2020. Long-term conservation tillage and
846 nitrogen fertilization effects on soil aggregate distribution, nutrient stocks and enzymatic
847 activities in bulk soil and occluded microaggregates. Soil and Tillage Research 196, 104482.

Pittelkow, C.M., Liang, X., Linquist, B.A., Van Groenigen, K.J., Lee, J., Lundy, M.E., van Gestel, N., Six, J., Venterea R.T., van Kessel, C., 2015. Productivity limits and potentials of the principles of conservation agriculture. Nature 517, 365–368.

Pulleman, M.M., Six, J., Uyl, A., Marinissen. J.C.Y., Jongmans, A.G., 2005. Earthworms and management affect organic matter incorporation and microaggregate formation in agricultural soils. Applied Soil Ecology 29, 1–15.

Quast, C., Pruesse, E., Yilmaz, P., Gerken, J., Schweer, T., Yarza, P., et al., 2012. The SILVA ribosomal RNA gene database project: improved data processing and web-based tools. Nucleic Acids Research 41, D590–D596.

Rillig, M.C., Aguilar-Trigueros, C.A., Bergmann, J., Verbruggen, E., Veresoglou, S.D., Lehmann, A., 2015. Plant root and mycorrhizal fungal traits for understanding soil aggregation. New Phytologist 205, 1385–1388.

Rillig, M.C., Mummey, D.L., 2006. Mycorrhizas and soil structure. New Phytologist 171, 41–53.

Rillig, M.C., Wright, S.F., Eviner, V.T., 2002. The role of arbuscular mycorrhizal fungi and glomalin in soil aggregation: comparing effects of five plant species. Plant and Soil 238, 325–333.

Rusinamhodzi, L., Corbeels, M., Van Wijk, M.T., Rufino, M.C., Nyamangara, J., Giller, K.E., 2011. A meta-analysis of long-term effects of conservation agriculture on maize grain yield under rain-fed conditions. Agronomy for Sustainable Development 31, 657.

Santos, S.S., Schöler, A., Nielsen, T.K., Hansen, L.H., Schloter, M., Winding, A., 2020. Land use as a driver for protist community structure in soils under agricultural use across Europe. Science of the Total Environment 717, 137228.

Schmidt, M.W., Torn, M.S., Abiven, S., Dittmar, T., Guggenberger, G., Janssens, I.A., Kleber, M., Kögel-Knabner, I., Lehmann, J., Manning, D.A.C., Nannipieri, P., Rasse, D.P., Steve Weiner, S., Susan E. Trumbore, S.E., 2011. Persistence of soil organic matter as an ecosystem property. Nature 478, 49–56.

874 Schoch, C. L., Seifert, K. A., Huhndorf, S., Robert, V., Spouge, J. L., Levesque, C. A., Chen, W.,
875 Fungal Barcoding Consortium, 2012. Nuclear ribosomal internal transcribed spacer (ITS)
876 region as a universal DNA barcode marker for Fungi. Proceedings of the National Academy of
877 Sciences 109, 6241-6246.
878 Sheehy, J., Regina, K., Alakukku, L., Six, J., 2015. Impact of no-till and reduced tillage on
879 aggregation and aggregate-associated carbon in Northern European agroecosystems. Soil and
880 Tillage Research 150, 107–113.
881 Siddiky, M.R.K., Kohler, J., Cosme, M., Rillig, M.C., 2012a. Soil biota effects on soil structure:
882 Interactions between arbuscular mycorrhizal fungal mycelium and collembola. Soil Biology
883 and Biochemistry 50, 33–39.
884 Siddiky, M.R.K., Schaller, J., Caruso, T., Rillig, M.C., 2012b. Arbuscular mycorrhizal fungi and
885 Collembola non-additively increase soil aggregation. Soil Biology and Biochemistry 47, 93–99.
886 Six, J., Bossuyt, H., Degryze, S., Denef, K., 2004. A history of research on the link between (micro)
887 aggregates, soil biota, and soil organic matter dynamics. Soil and Tillage Research 79, 7–31.
888 Six, J., Elliott, E.T., Paustian, K., 1999. Aggregate and soil organic matter dynamics under
889 conventional and no-tillage systems. Soil Science Society of America Journal 63, 1350–1358.
890 Six, J., Elliott, E.T., Paustian, K., 2000. Soil macroaggregate turnover and microaggregate
891 formation: a mechanism for C sequestration under no-tillage agriculture. Soil Biology and
892 Biochemistry 32, 2099–2103.
893 Six, J., Paustian, K., 2014. Aggregate-associated soil organic matter as an ecosystem property and a
894 measurement tool. Soil Biology and Biochemistry 68, A4–A9.
895 Soil Survey Staff, 1975. Soil taxonomy. A Basic System of Soil Classification for Making and
896 Interpreting Soil Surveys. USDA-SCS Agrjic. Handb.: Washington, DC, USA.
897 Stoeck, T., Bass, D., Nebel, M., Christen, R., Jones, M.D., Breiner, H.W., Richards, T.A., 2010.
898 Multiple marker parallel tag environmental DNA sequencing reveals a highly complex
899 eukaryotic community in marine anoxic water. Molecular Ecology 19, 21–31.

900 Sun, A., Jiao, X.Y., Chen, Q., Trivedi, P., Li, Z., Li, F., Zheng, Y., Lin, Y., Hu, H.W. He, J.-Z.,
901 2021. Fertilization alters protistan consumers and parasites in crop-associated microbiomes.
902 Environmental Microbiology 23, 2169–2183.
903 ter Braak, C.J.F., Schaffers, A.P., 2004. Co-correspondence analysis: a new ordination method to
904 relate two community compositions. Ecology 85, 834–846.
905 ter Braak, C.J.F., Smilauer, P., 2012. Canoco reference manual and user's guide: software for
906 ordination (version 5.0). Microcomputer Power: Ithaca, USA.
907 Tipton, L., Müller, C.L., Kurtz, Z.D., Huang, L., Kleerup, E., Morris, A., Bonneau, R., Ghedin., E.,
908 2018. Fungi stabilize connectivity in the lung and skin microbial ecosystems. Microbiome 6,
909 12.
910 Tisdall, J.M., Oades, J., 1982. Organic matter and water-stable aggregates in soils. European
911 Journal of Soil Science 33, 141–163.
912 Totsche, K.U., Amelung, W., Gerzabek, M.H., Guggenberger, G., Klumpp, E., Knief, C.,
913 Lehndorff, E., Mikutta, R., Peth, S., Prechtel, A., Ray, N., Kögel-Knabner, I., 2018.
914 Microaggregates in soils. Journal of Plant Nutrition and Soil Science 181, 104–136.
915
916
917 van Capelle, C., Schrader, S., & Brunotte, J., 2012. Tillage-induced changes in the functional
918 diversity of soil biota–A review with a focus on German data. European Journal of Soil
919 Biology 50, 165-181.
920 Wagg, C., Schlaeppi, K., Banerjee, S., Kuramae, E.E., van der Heijden, M.G., 2019. Fungal-
921 bacterial diversity and microbiome complexity predict ecosystem functioning. Nature
922 Communication 10, 1–10.
923 Wang, Q., Ma, M., Jiang, X., Guan, D., Wei, D., Zhao, B., Chen, S., Cao, F., Li, L., Yang, X., Li,
924 J., 2019. Impact of 36 years of nitrogen fertilization on microbial community composition and

soil carbon cycling-related enzyme activities in rhizospheres and bulk soils in northeast China. Applied Soil Ecology 136, 148–157.

Wang, X., Bian, Q., Jiang, Y., Zhu, L., Chen, Y., Liang, Y., Sun, B., 2021. Organic amendments drive shifts in microbial community structure and keystone taxa which increase C mineralization across aggregate size classes. Soil Biology and Biochemistry 153, 108062.

Wickham, H., Chang, W., 2008. ggplot2: An implementation of the Grammar of Graphics. R package version 0.7.

Xiong, C., Zhu, Y.G., Wang, J.T., Singh, B., Han, L.L., Shen, J.P., Li, P. Wang, G., Wu, C., Ge, A., Zhang, L., He, J., 2021. Host selection shapes crop microbiome assembly and network complexity. New Phytologist 229, 1091–1104.

Yilmaz, P., Parfrey, L.W., Yarza, P., Gerken, J., Pruesse, E., Quast, C., et al., 2013. The SILVA and "all-species living tree project (LTP)" taxonomic frameworks. Nucleic Acids Research 42, D643–D648.

Zhang, S., Li, Q., Lü, Y., Zhang, X., Liang, W., 2013. Contributions of soil biota to C sequestration varied with aggregate fractions under different tillage systems. Soil Biology and Biochemistry 62, 147–156.

Zhang, X., Li, Q., Zhu, A., Liang, W., Zhang, J., Steinberger, Y., 2012. Effects of tillage and residue management on soil nematode communities in North China. Ecological Indicators 13, 75–81.

Zhang, Z., Zhang, X., Mahamood, M., Zhang, S., Huang, S., Liang, W., 2016. Effect of long-term combined application of organic and inorganic fertilizers on soil nematode communities within aggregates. Scientific Report 6, 31118.

Zhao, Z.B., He, J.Z., Geisen, S., Han, L.L., Wang, J.T., Shen, J.P., Wei, W., Fang, Y., Li, P., Zhang, L., 2019. Protist communities are more sensitive to nitrogen fertilization than other microorganisms in diverse agricultural soils. Microbiome 7, 1–16.

951 **Figure captions**

952

953 **Fig. 1.** Long-term effect of conservation management on community composition of eukaryotes in
954 two soil matrices: small macroaggregates (sM) and occluded microaggregates (mM). Managements
955 were: MTN0 (minimum tillage and 0 kg N $ha^{-1}$), MTN200 (MT and 200 kg N $ha^{-1}$), CTN0
956 (conventional tillage and 0 kg N $ha^{-1}$) and CTN200 (CT and 200 kg N $ha^{-1}$). Neighbor-joining (NJ)
957 tree of 56 eukaryotic taxon representative sequences (classes) found in (a) sM and (d) mM. NJ trees
958 are based on the sequences obtained from the amplification of the V4 region (18 SSU rRNA gene).
959 The eukaryotic taxa were assigned to Operational Taxonomic Unit (OTU) (at class phylogenetic
960 resolution) by BLAST against the 18S SSU SILVA database by clustering sequence reads at the
961 97% similarity threshold. For each OTU, the proportion of sequences retrieved in each management
962 (MTN0, light green; MTN200, dark green; CTN0, light red; CTN200, dark red) and soil depth (0–
963 15 cm: light grey; 15–30 cm: dark grey) are shown in the pie charts. Venn diagrams of eukaryotic
964 classes uniquely retrieved and shared across managements in sM at (b) 0-15 cm and (c) at 15-30
965 cm, and in mM at (e) 0-15 cm and (f) at 15-30 cm.

966

967 **Fig. 2.** Long-term effect of conservation management on relative abundances and community
968 structures of eukaryotes in two soil matrices: small macroaggregates (sM) and occluded
969 microaggregates (mM). Managements were: MTN0 (minimum tillage and 0 kg N $ha^{-1}$), MTN200
970 (MT and 200 kg N $ha^{-1}$), CTN0 (conventional tillage and 0 kg N $ha^{-1}$) and CTN200 (CT and 200 kg
971 N $ha^{-1}$). (a) Relative abundances of eukaryotes at phylum level across treatments, matrices and soil
972 depths. (b) Principal Coordinates Analysis (PCO) biplots on the interaction of tillage and N
973 fertilization on the eukaryotic community structure at class level in sM at 0-15 cm and (c) at 15-30
974 cm, and (d) in mM at 0-15 cm. The output of the PCO biplots is based on the significant effect of

975 treatments following the permutational analysis of variance (PERMANOVA). We displayed only
976 the taxa with a strong correlation (r = 0.50-0.70) with the ordination scores on each PCO axis.

977

978 **Fig. 3.** Venn diagrams of eukaryotic phyla uniquely retrieved and shared in sM and mM at 0-15 cm
979 (a) and at 15-30 cm (b). Principal Coordinates Analysis (PCO) biplots on effect of soil matrix
980 (small macroaggregates sM *vs* occluded microaggregates mM) on eukaryotic community structure
981 at phylum resolution at (a) 0-15 cm and at (b) 15-30 cm soil depth. The PCO biplots are based on
982 the significant effect of soil matrix according to the permutational analysis of variance
983 (PERMANOVA). In the biplots, only the taxa with a strong correlation (r = 0.50-0.70) with the
984 ordination scores on each PCO axis were displayed.

985

986 **Fig. 4.** Eukaryotic networks (within-domain networks) and eukaryotic-prokaryotic networks (cross-
987 domain Associations networks) (at class phylogenetic resolution) in small macroaggregates (sM)
988 (a,b) and occluded microaggregates (mM) (c,d) at surface layer (0-15 cm soil depth). Within-
989 domain networks were built using the SParse InversE Covariance estimation for Ecological
990 ASsociation Inference (SPIEC-EASI) package version 0.1 in R
991 (https://github.com/zdk123/SpiecEasi/), while cross-domain networks were built by the cross-
992 domain extension of SPIEC-EASI (Kurtz et al., 2015; Tipton et al., 2018). Details about network
993 construction are given in Material and Methods and Supplementary Methods 3, and R scripts are
994 provided in Supplementary Methods 4.

**Table 1**

Results of PERMANOVA and variation partitioning of the long-term effect of conservation management (tillage and N fertilization) within small macroaggregates (sM) and occluded microaggregates (mM) and of the effect of matrix (sM *vs* mM) on eukaryotic community structure at 0-15 and 15-30 cm soil depths.

| | df | Pseudo-F | P (perm) | Variance explained | df | Pseudo-F | P (perm) | Variance explained |
|---|---|---|---|---|---|---|---|---|
| | | | 0-15 cm | | | | 15-30 cm | |
| *Eukaryotes at class level - sM* | | | | | | | | |
| TIL[†] | 1 | 2.24 | **0.025**[‡] | **11.96** | 1 | 4.02 | **0.003** | **22.69** |
| N fert | 1 | 2.11 | **0.017** | **10.76** | 1 | 2.21 | **0.012** | **9.05** |
| TIL x N fert | 1 | 1.99 | **0.024** | **19.13** | 1 | 2.55 | **0.019** | **23.20** |
| *PERMDISP* | | | | | | | | |
| TIL | | | 0.693 | | | | 0.071 | |
| N fert | | | 0.078 | | | | 0.359 | |
| *Eukaryotes at class level - mM* | | | | | | | | |
| TIL | 1 | 4.60 | **0.003** | **19.94** | 1 | 1.05 | 0.411 | - |
| N fert | 1 | 3.90 | **0.002** | **16.02** | 1 | 1.64 | 0.127 | - |
| TIL x N fert | 1 | 3.79 | **0.006** | **30.85** | 1 | 0.90 | 0.569 | - |
| *PERMDISP* | | | | | | | | |
| TIL | | | 0.237 | | | | - | |
| N fert | | | 0.362 | | | | - | |
| *Eukaryotes at phylum level - sM vs mM* | | | | | | | | |
| Matrix[§] | 1 | 1.07 | **0.001** | **38.31** | 1 | 11.18 | **0.001** | **42.51** |
| TIL x N fert | 1 | 2.90 | **0.004** | **3.74** | 1 | 1.22 | 0.287 | 4.51 |
| N fert | 1 | 1.54 | 0.140 | 10.69 | 1 | 2.36 | **0.014** | **2.84** |
| *PERMDISP* | | | | | | | | |
| Matrix | | | **0.025** | | | | 0.069 | |

[†]PERMANOVA was performed following a split-plot design with tillage (TIL) as main-plot factor and N fertilization (N fert) as subplot factor and with three replicate plots per treatment: TIL (minimum tillage and conventional tillage) and N fert (0 kg N $ha^{-1}$ and 200 kg N $ha^{-1}$).

[‡]In bold statistically significant values ($P \leq 0.05$).

[§]PERMANOVA was performed using the matrix as fixed factor, TIL and N fert as covaribales and 12 replicate plots per matrix.

**Table 2**
Traits of within- (eukaryotes) and cross-domain (eukaryotes - prokaryotes) network in macroaggregates (sM) and occluded microaggregates (mM) at 0-15 and 15-30 cm soil depth (for the network diagrams see Fig. 4 and S10).

| Traits | sM 0-15 | sM 15-30 | mM 0-15 | mM 15-30 |
|---|---|---|---|---|
| *Eukaryotes* | | | | |
| Number of nodes excluding singletons | 37 | 33 | 46 | 39 |
| Number of edges | 29 | 25 | 44 | 31 |
| Number of singletons | 12 | 16 | 8 | 15 |
| Number of dyads | 3 | 6 | 1 | 6 |
| Number of subnetworks | 6 | 5 | 4 | 5 |
| Mean nodes per subnetwork | 5.17 ± 0.60 | 4.20 ± 0.49 | 11.0 ± 7.34 | 5.40 ± 1.03 |
| Linkage density (complexity) | 1.57 ± 0.11 a | 1.51 ± 0.13 | 1.89 ± 0.14 b | 1.56 ± 0.13 |
| % Positive interactions | 78.4 | 75.8 | 95.7 | 79.5 |
| Modularity | 3 | 5 | 4 | 5 |
| Identity of phyla with a frequency within the subnetworks ≥ 10% | Basidiomycota 15.9% Cercozoa 16.8% | Ascomycota 20% Basidiomycota 10% Cercozoa 11.7% | Cercozoa 11.6% Ochrophyta 16.7% | Chlorophyta 12% Cercozoa 21.7% Stramenopiles 16.7% |
| *Eukaryotes - Prokaryotes* | | | | |
| Total number of nodes excluding singletons | 79 | 83 | 96 | 67 |
| Number of eukaryotic nodes excluding singletons | 37 | 38 | 49 | 30 |
| Number of prokaryotic nodes excluding singletons | 42 | 45 | 47 | 37 |
| Number of edges | 74 | 72 | 109 | 54 |
| Number of singletons | 22 | 18 | 6 | 36 |
| Number of dyads | 3 | 8 | 2 | 5 |
| Number of subnetworks | 7 | 4 | 8 | 11 |
| Mean nodes per subnetwork | 10.43 ± 4.43 | 8.38 ± 2.74 | 23.50 ± 19.50 | 5.18 ± 0.70 |
| Linkage density (complexity) | 1.87 ± 0.11 a | 1.76 ± 0.11 | 2.26 ± 0.12 b | 1.61 ± 0.11 |
| Modularity | 9 | 9 | 11 | 9 |
| Percentage of eukaryotes per subnetwork | 68.39 ± 12.26 | 50.79 ± 12.03 | 74.70 ± 14.61 | 39.01 ± 14.69 |
| Percentage of prokaryotes per subnetwork | 31.61 ± 12.26 | 49.21 ± 12.03 | 25.30 ± 14.61 | 60.99 ± 14.69 |
| Number of subnetworks with only eukaryotes | 2 | 1 | 2 | 4 |
| Number of subnetworks with only prokaryotes | 0 | 1 | 0 | 5 |
| Number of mixed subnetworks | 5 | 6 | 2 | 2 |

**Table 3**
Traits of within- (eukaryotes) and cross-domain (eukaryotes - prokayotes) network in macroaggregates (sM) and occluded microaggregates (mM) at 0-15 and 15-30 cm soil depth (for the network diagrams see Fig. 4 and S10).

| Traits | sM 0-15 | sM 15-30 | mM 0-15 | mM 15-30 |
|---|---|---|---|---|
| *Eukaryotes* | | | | |
| Number of nodes excluding singletons | 37 | 33 | 46 | 39 |
| Number of edges | 29 | 25 | 44 | 31 |
| Number of singletons | 12 | 16 | 8 | 15 |
| Number of dyads | 3 | 6 | 1 | 6 |
| Number of subnetworks | 6 | 5 | 4 | 5 |
| Mean nodes per subnetwork | 5.17 ± 0.60 | 4.20 ± 0.49 | 11.0 ± 7.34 | 5.40 ± 1.03 |
| Linkage density (complexity) | 1.57 ± 0.11 a | 1.51 ± 0.13 | 1.89 ± 0.14 b | 1.56 ± 0.13 |
| % Positive interactions | 78.4 | 75.8 | 95.7 | 79.5 |
| Modularity | 3 | 5 | 4 | 5 |
| Identity of phyla with a frequency within the subnetworks ≥ 10% † | Basidiomycota 15.9% Cercozoa 16.8% | Ascomycota 20% Basidiomycota 10% Cercozoa 11.7% | Cercozoa 11.6% Ochrophyta 16.7% | Chlorophyta 12% Cercozoa 21.7% Stramenopiles 16.7% |
| *Eukaryotes - Prokaryotes* | | | | |
| Total number of nodes excluding singletons | 79 | 83 | 96 | 67 |
| Number of eukaryotic nodes excluding singletons | 37 | 38 | 49 | 30 |
| Number of prokaryotic nodes excluding singletons | 42 | 45 | 47 | 37 |
| Number of edges | 74 | 72 | 109 | 54 |
| Number of singletons | 22 | 18 | 6 | 36 |
| Number of dyads | 3 | 8 | 2 | 5 |
| Number of subnetworks | 7 | 4 | 8 | 11 |
| Mean nodes per subnetwork | 10.43 ± 4.43 | 8.38 ± 2.74 | 23.50 ± 19.50 | 5.18 ± 0.70 |
| Linkage density (complexity) | 1.87 ± 0.11 a | 1.76 ± 0.11 | 2.26 ± 0.12 b | 1.61 ± 0.11 |
| Modularity | 9 | 9 | 11 | 9 |
| Percentage of eukaryotes per subnetwork | 68.39 ± 12.26 | 50.79 ± 12.03 | 74.70 ± 14.61 | 39.01 ± 14.69 |
| Percentage of prokaryotes per subnetwork | 31.61 ± 12.26 | 49.21 ± 12.03 | 25.30 ± 14.61 | 60.99 ± 14.69 |
| Number of subnetworks with only eukaryotes | 2 | 1 | 2 | 4 |
| Number of subnetworks with only prokaryotes | 0 | 1 | 0 | 5 |
| Number of mixed subnetworks | 5 | 6 | 2 | 2 |

† For details about the traits of within-domain networks for each eukaryotic phylum occurring in sM and mM at both soil depths see Table S5.

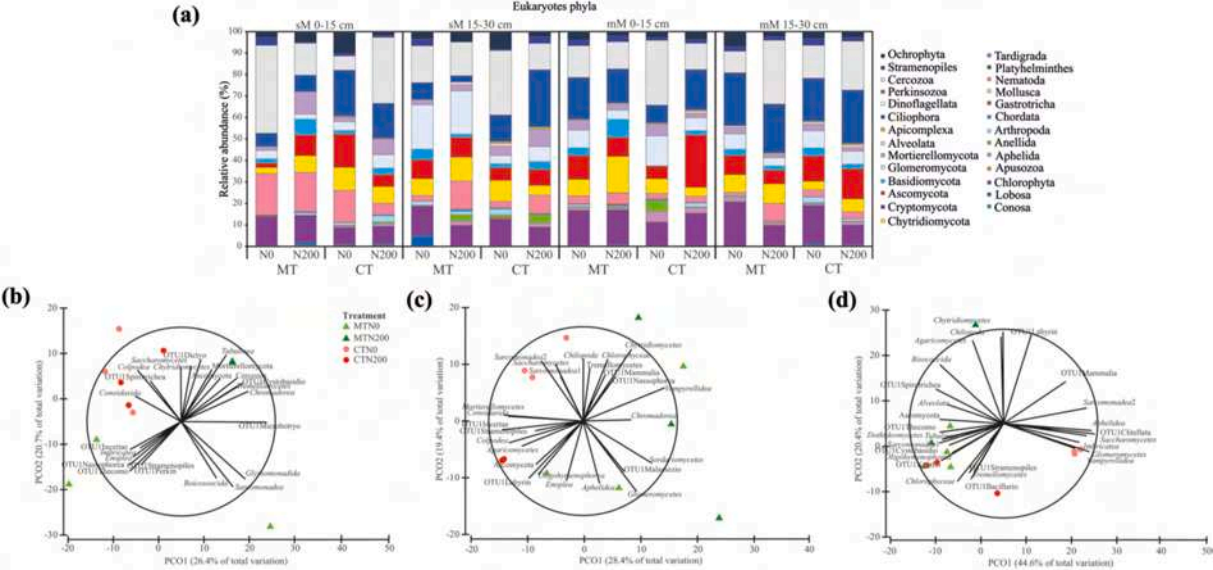
(a)
Eukaryotes phyla
sM 0-15 cm
sM 15-30 cm
mM 0-15 cm
mM 15-30 cm
Relative abundance (%)
N0
N200
MT
CT
Ochrophyta
Stramenopiles
Cercozoa
Perkinsozoa
Dinoflagellata
Ciliophora
Apicomplexa
Alveolata
Mortierellomycota
Glomeromycota
Basidiomycota
Ascomycota
Cryptomycota
Chytridiomycota
Tardigrada
Platyhelminthes
Nematoda
Mollusca
Gastrotricha
Chordata
Arthropoda
Anellida
Aphelida
Apusozoa
Chlorophyta
Lobosa
Conosa
(b)
(c)
(d)
Treatment
MTN0
MTN200
CTN0
CTN200
PCO1 (26.4% of total variation)
PCO2 (20.7% of total variation)
PCO1 (28.4% of total variation)
PCO2 (19.4% of total variation)
PCO1 (44.6% of total variation)
PCO2 (20.4% of total variation)

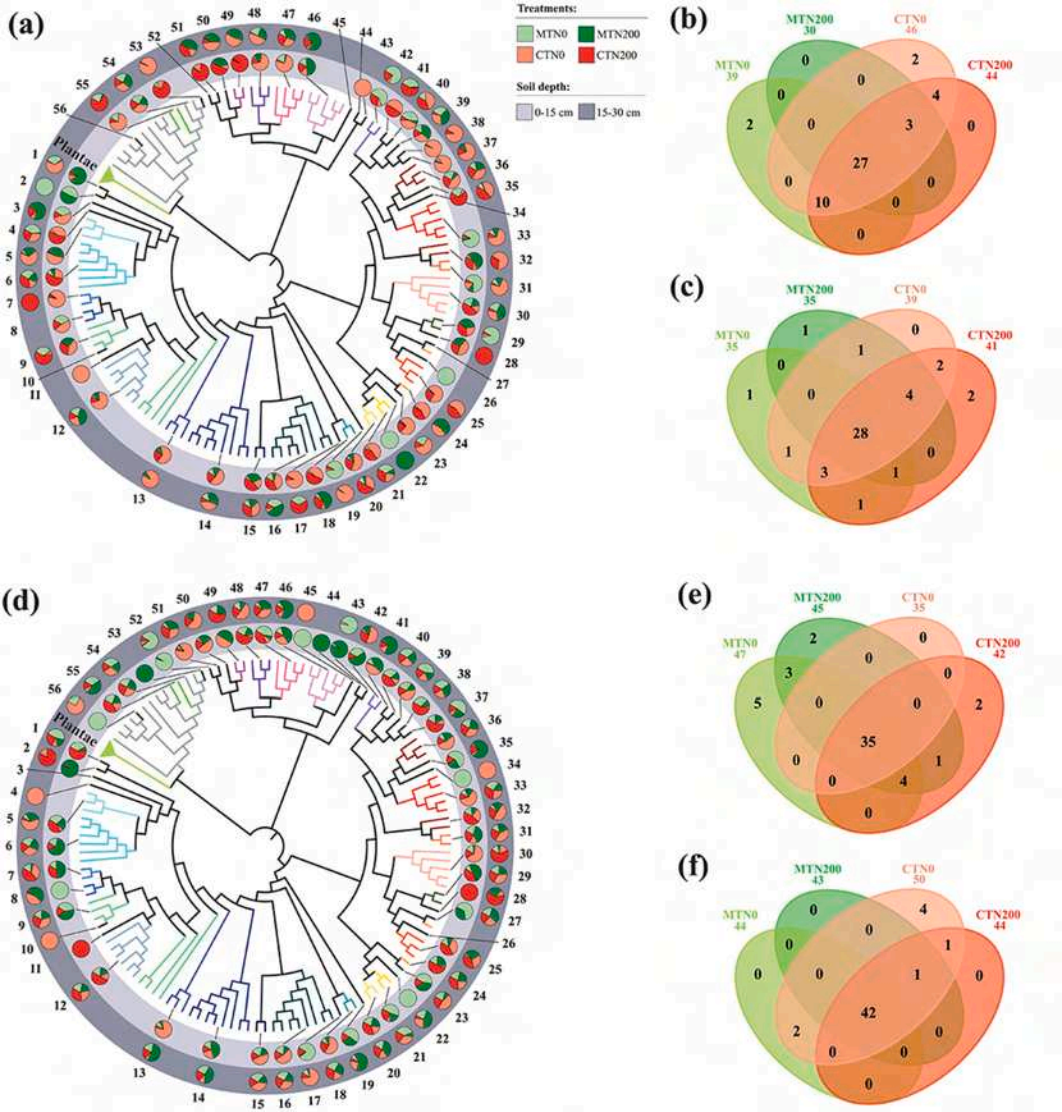
(a)
Treatments:
MTN0
MTN200
CTN0
CTN200
Soil depth:
0-15 cm
15-30 cm
Plantae
(b)
MTN200
30
CTN0
46
MTN0
39
CTN200
44
0
0
2
0
0
4
2
0
3
0
27
0
0
10
0
0
(c)
MTN200
35
CTN0
39
MTN0
35
CTN200
41
1
0
1
0
2
1
0
4
2
28
1
3
0
1
1
(d)
Plantae
(e)
MTN200
45
CTN0
35
MTN0
47
CTN200
42
2
0
3
0
0
5
0
0
2
35
0
0
1
4
0
(f)
MTN200
43
CTN0
50
MTN0
44
CTN200
44
0
0
4
0
0
1
0
0
1
0
42
2
0
0
0
0
Eukaryotic taxa:
1. Cystobasidiomycetes
2. Microbotryomycetes
3. Malasseziomycetes
4. Exobasidiomycetes
5. Tremellomycetes
6. Agaricomycetes
7. Dothideomycetes
8. Eurotiomycetes
9. Ascomycota
10. Lecanoromycetes
11. Pezizomycetes
12. Sordariomycetes
13. Saccharomycetes
14. Chytridiomycetes
15. Mortierellomycota
16. Glomeromycetes
17. Cryptomycota
18. Aphelidea
19. Thecomonadea
20. Colpodea
21. Oligohymenophorea
22. Nassophorea
23. Spirotrichea
24. Alveolata
25. Conoidasida
26. Perkinsea
27. Dinophyceae
28. Dictyostelia
29. Tubulinea
30. Vampyrellidea
31. Sarcomonadea1
32. Cercozoa
33. Sarcomonadea2
34. Thecofilosea
35. Incertae sedis
36. Imbricatea
37. Bacillariophyceae
38. Xanthophyceae
39. Chrysophyceae
40. Stramenopiles
41. Labyrinthulomycetes
42. Bolcosoecida
43. Gastrotricha
44. Rhabditophora
45. Eutardigrada
46. Chromadorea
47. Enoplea
48. Arachnida
49. Chilopoda
50. Mammalia
51. Clitellata
52. Gastropoda
53. Ulvophyceae
54. Chlorophyceae
55. Trebouxiophyceae
56. Chlorophyta

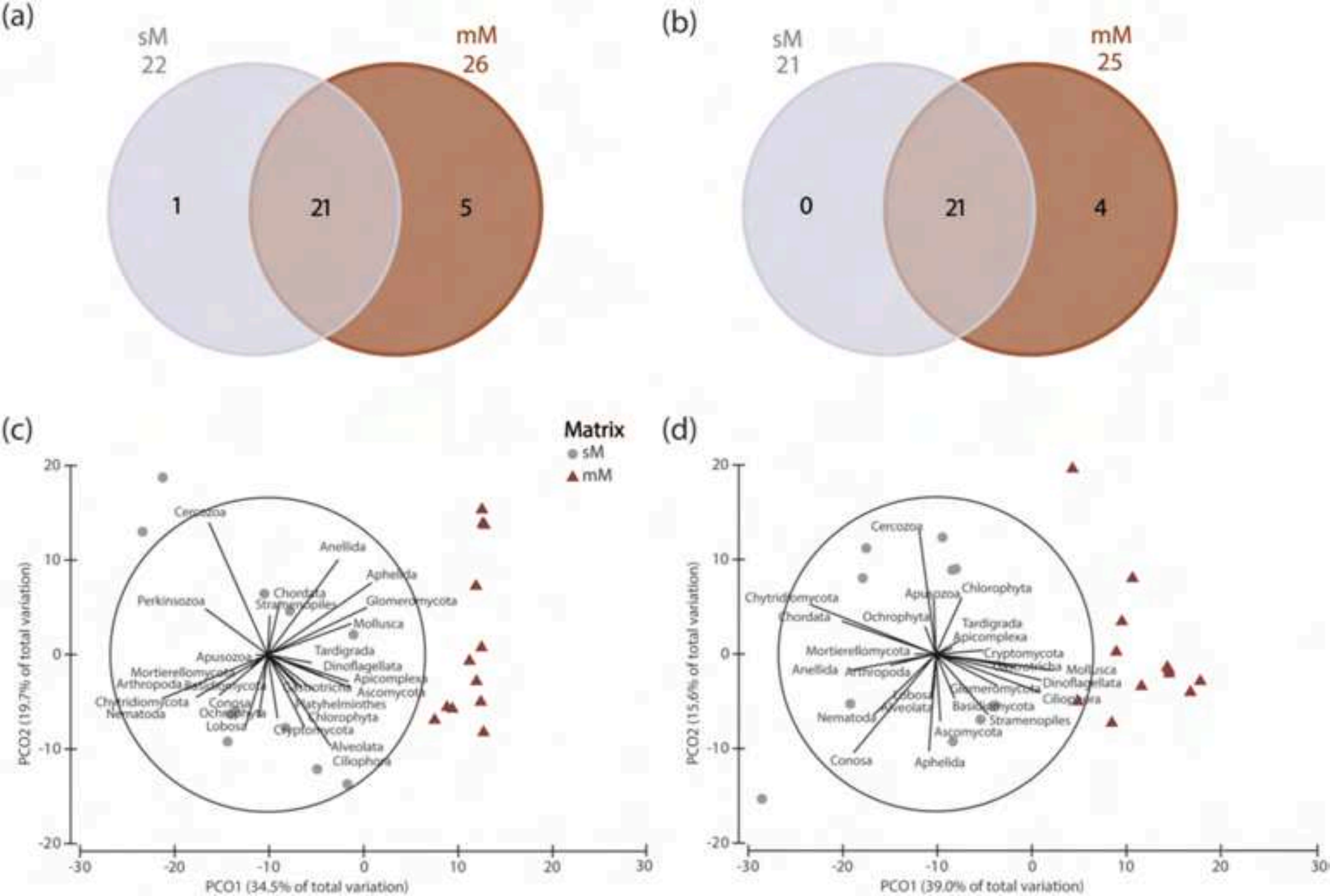
(a)
sM
22
mM
26
1
21
5
(b)
sM
21
mM
25
0
21
4
(c)
Matrix
sM
mM
PCO2 (19.7% of total variation)
PCO1 (34.5% of total variation)
Cercozoa
Anellida
Aphelida
Chordata
Stramenopiles
Perkinsozoa
Glomeromycota
Mollusca
Tardigrada
Apusozoa
Dinoflagellata
Mortierellomycota
Arthropoda
Apicomplexa
Basidiomycota
Ascomycota
Chytridiomycota
Conosa
Platyhelminthes
Nematoda
Ochrophyta
Chlorophyta
Lobosa
Cryptomycota
Alveolata
Ciliophora
(d)
PCO2 (15.6% of total variation)
PCO1 (39.0% of total variation)
Cercozoa
Chytridiomycota
Apusozoa
Chlorophyta
Chordata
Ochrophyta
Tardigrada
Apicomplexa
Mortierellomycota
Cryptomycota
Anellida
Arthropoda
Mollusca
Dinoflagellata
Glomeromycota
Lobosa
Ciliophora
Alveolata
Basidiomycota
Nematoda
Stramenopiles
Ascomycota
Conosa
Aphelida

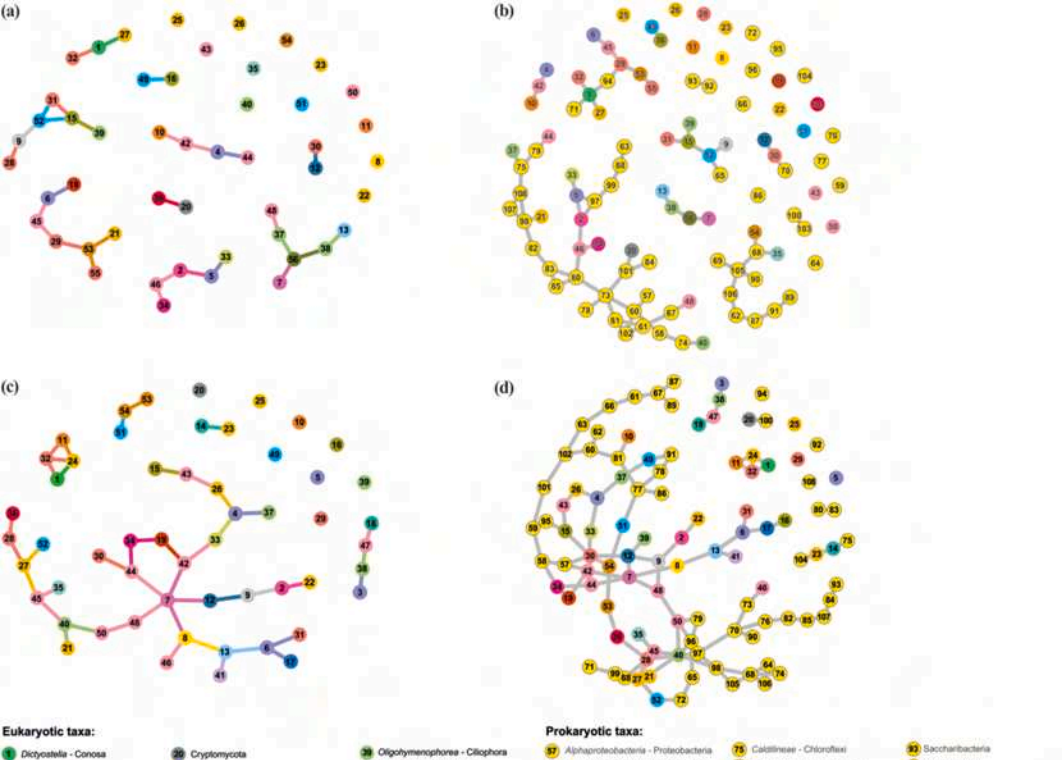


**Eukaryotic taxa:**

1. *Dictyostelia* - Conosa
2. *Tubulinea* - Lobosa
3. Chlorophyta
4. *Chlorophyceae* - Chlorophyta
5. *Trebouxiophyceae* - Chlorophyta
6. *Ulvophyceae* - Chlorophyta
7. *Thecomonadea* - Apusozoa
8. *Aphelidea* - Aphelida
9. *Clitellata* - Anellida
10. *Arachnida* - Arthropoda
11. *Chilopoda* - Arthropoda
12. *Mammalia* - Chordata
13. Gastrotricha
14. *Gastropoda* - Mollusca
15. *Chromadorea* - Nematoda
16. *Enoplea* - Nematoda
17. *Rhabditophora* - Platyhelminthes
18. *Eutardigrada* - Tardigrada
19. *Chytridiomycetes* - Chytridiomycota
20. Cryptomycota
21. Ascomycota
22. *Dothideomycetes* - Ascomycota
23. *Eurotiomycetes* - Ascomycota
24. *Lecanoromycetes* - Ascomycota
25. *Pezizomycetes* - Ascomycota
26. *Sordariomycetes* - Ascomycota
27. *Saccharomycetes* - Ascomycota
28. *Agaricomycetes* - Basidiomycota
29. *Tremellomycetes* - Basidiomycota
30. *Cystobasidiomycetes* - Basidiomycota
31. *Microbotryomycetes* - Basidiomycota
32. *Exobasidiomycetes* - Basidiomycota
33. *Glomeromycetes* - Glomeromycota
34. *Mortierellomycetes* - Mortierellomycota
35. Alveolata
36. *Conoidiasida* - Apicomplexa
37. *Colpodea* - Ciliophora
38. *Nassophorea* - Ciliophora
39. *Oligohymenophorea* - Ciliophora
40. *Spirotrichea* - Ciliophora
41. Dinoflagellata
42. *Sarcomonadea1* - Cercozoa
43. *Sarcomonadea2* - Cercozoa
44. *Imbricatea* - Cercozoa
45. Incertae sedis - Cercozoa
46. Cercozoa - Cercozoa
47. *Thecofilosea* - Cercozoa
48. *Vampyrellidea* - Cercozoa
49. Stramenopiles
50. *Bicosoecida* - Cercozoa
51. *Labyrinthulomycetes* - Stramenopiles
52. *Chrysophyceae* - Stramenopiles
53. *Bacillariophyceae* - Ochrophyta
54. *Xanthophyceae* - Ochrophyta
55. *Malasseziomycetes* - Basidiomycota
56. *Perkinsea* - Perkinsozoa

**Prokaryotic taxa:**

57. *Alphaproteobacteria* - Proteobacteria
58. *Deltaproteobacteria* - Proteobacteria
59. *Gammaproteobacteria* - Proteobacteria
60. *Betaproteobacteria* - Proteobacteria
61. *Blastocatellia* - Acidobacteria
62. Acidobacteria
63. *Holophagae* - Acidobacteria
64. Chlamydiae
65. *Clostridia* - Firmicutes
66. *Bacilli* - Firmicutes
67. Gemmatimonadetes
68. Cloacimonetes
69. *Sprochaetia* - Spirochaetes
70. *Deinococci* - Deinococcus Thermus
71. *Anaerolineae* - Chloroflexi
72. *Dehalococcoidia* - Chloroflexi
73. Chloroflexi
74. *Ardenticatenia* - Chloroflexi
75. *Caldilineae* - Chloroflexi
76. *Kiritimatiellae* - Verrucomicrobia
77. *Chloroflexia* - Chloroflexi
78. *Thermomicrobia* - Chloroflexi
79. *Elusimicrobia* - Elusimicrobia
80. *Thermoleophilia* - Actinobacteria
81. Actinobacteria 1
82. *Rubrobacteria* - Actinobacteria
83. *Acidimicrobiia* - Actinobacteria
84. *Nitriliruptoria* - Actinobacteria
85. Actinobacteria 2
86. Verrucomicrobiae - Verrucomicrobia
87. Verrucomicrobia
88. *Spartobacteria* - Verrucomicrobia
89. *Phycisphaerae* - Planctomycetes
90. Planctomycetes
91. *Planctomycetacia* - Planctomycetes
92. Omnitrophica
93. Saccharibacteria
94. Parcubacteria
95. Peregrinibacteria
96. Cyanobacteria
97. Chlorobia - Chlorobi
98. *Ignavibacteria* - Chlorobi
99. *Cytophagia* - Bacteroidetes
100. Bacteroidetes
101. *Flavobacteriia* - Bacteroidetes
102. *Sphingobacteriia* - Bacteroidetes
103. Candidatus Berkelbacteria
104. Microgenomates
105. *Methanobacteria* - Euryarchaeota
106. *Methanomicrobia* - Euryarchaeota
107. Thermoplasmata - Euryarchaeota
108. Thaumarchaeota

**Highlights**

- Eukaryote diversity responded differently to managements across soil aggregates
- A core community of eukaryotes was found across managements, aggregates and depths
- Tillage shifted eukaryotic structure in sM and mM according to N availability
- Protists and fungi positively correlated with the amount of sM, mM and SOC content
- Within- and cross-domain networks of mM at 0-15 cm showed the highest complexity

**Declaration of interests**

☒ The authors declare that they have no known competing financial interests or personal relationships that could have appeared to influence the work reported in this paper.

☐The authors declare the following financial interests/personal relationships which may be considered as potential competing interests: